

REPUBLIC OF TÜRKİYE
YILDIZ TECHNICAL UNIVERSITY
GRADUATE SCHOOL OF SCIENCE AND ENGINEERING

**AXISYMMETRIC BENDING ANALYSIS OF ANNULAR
PLATES**

Bensu ÇÖL

MASTER OF SCIENCE THESIS

Department of Civil Engineering

Mechanics Program

Supervisor

Prof. Dr. Murat ALTEKİN

August 2023

REPUBLIC OF TÜRKİYE
YILDIZ TECHNICAL UNIVERSITY
GRADUATE SCHOOL OF SCIENCE AND ENGINEERING

**AXISYMMETRIC BENDING ANALYSIS OF ANNULAR
PLATES**

A thesis submitted by Bensu ÇÖL in partial fulfillment of the requirements for the degree of MASTER OF SCIENCE is approved by the committee on 07.08.2023 in Department of Civil Engineering, Mechanics Program.

Prof. Dr. Murat ALTEKİN
Yıldız Technical University
Supervisor

Approved By the Examining Committee

Prof. Dr. Murat ALTEKİN, Supervisor
Yıldız Technical University

Doç. Dr. Yıldırım Serhat ERDOĞAN, Member
Yıldız Technical University

Dr. Öğr. Üye. Esra Eylem KARATAŞ, Member
Gaziantep University

I hereby declare that I have obtained the required legal permissions during data collection and exploitation procedures, that I have made the in-text citations and cited the references properly, that I haven't falsified and/or fabricated research data and results of the study and that I have abided by the principles of the scientific research and ethics during my Thesis Study under the title of Unified Effect of the Elastic Foundation and the Material Properties on the Nonlinear Bending Response of an Annular Plate supervised by my supervisor, Prof. Dr. Murat ALTEKİN. In the case of a discovery of false statement, I am to acknowledge any legal consequence.

Bensu ÇÖL

Signature



Dedicated to my father

ACKNOWLEDGEMENTS

Special thanks to my thesis supervisor Prof. Dr. Murat ALTEKİN, for his consistent support, patience, and feedbacks. His guidance and expertise have been essential in shaping this study.

I would also like to thank my family, and my friends for continuous encouragement throughout my study years.

Bensu ÇÖL



TABLE OF CONTENTS

LIST OF SYMBOLS	vi
LIST OF ABBREVIATIONS	viii
LIST OF FIGURES	ix
LIST OF TABLES	xi
ABSTRACT	xiii
ÖZET	xiv
1 INTRODUCTION	1
1.1 Literature Review.....	1
1.2 Objective of the Thesis	4
1.3 Hypothesis.....	4
2 ANALYSIS	5
2.1 Formulation.....	5
2.2 Variables and Governing Equations	6
2.3 Boundary Conditions	8
3 METHODOLOGY	9
3.1 Finite Difference Method.....	9
3.2 Newton-Raphson Method	9
4 ANALYSIS AND MODELING	10
4.1 Convergence Study and Validation of Results	10
4.2 Numerical Examples	14
4.3 Numerical Results	17
5 CONCLUSION	28
REFERENCES	29
A ADDITIONAL NUMERICAL RESULTS	35
PUBLICATIONS FROM THE THESIS	44

LIST OF SYMBOLS

m_r, m_θ	Bending moments
u, w	Displacement components
D	Flexural rigidity of plate
b	Inner radius of annular plate
M_r, M_θ	Nondimensional bending moments
W, U	Nondimensional deflection
K_{NW}	Nondimensional nonlinear Winkler parameter
N_r, N_θ	Nondimensional normal forces
W_{max}	Nondimensional maximum deflection
K_P	Nondimensional Pasternak parameter
Q	Nondimensional pressure load
X	Nondimensional radial coordinate
Q_r	Nondimensional shear force
K_W	Nondimensional Winkler parameter
k_{NW}	Nonlinear Winkler parameter
n_r, n_θ	Normal forces
N	Number of points (FDM)
λ, η	Orthotropy parameters
a	Outer radius of annular plate
k_P	Pasternak parameter
R	Parameter of radius
y	Parameter of thickness
h	Plate thickness
ν_r, ν_θ	Poisson's ratios
r	Radial coordinate
α	Ratio of inner radius to outer radius
ψ	Rotation
κ	Shear correction factor
q_r	Shear force

G_{rz}	Shear modulus
q	Uniform pressure load
k_w	Winkler parameter
E_θ, E_r	Young's moduli



LIST OF ABBREVIATIONS

BC	Boundary Condition
C	Clamped Edge
CPT	Classical Plate Theory
DR	Dynamic Relaxation Method
DQM	Differential Quadrature Method
DTM	Differential Transform Method
F	Free Edge
FDM	Finite Difference Method
FEM	Finite Element Method
FGM	Functionally Graded Material
FSDT	First Order Shear Deformation Theory
HSDT	Higher Order Shear Deformation Theory
L	Linear
MI	Isotropic Material
MO	Orthotropic Material
NL	Nonlinear
NR	Newton-Raphson Method
S	Simply Supported Edge
SSM	State Space Method

LIST OF FIGURES

Figure 2.1 Annular plate under transverse loading	5
Figure 3.1 FDM grid	9
Figure 4.1 Model of the annular plate (ANSYS).....	13
Figure 4.2 Deformed form of the annular C-C plate (ANSYS).....	13
Figure 4.3 Maximum deflection for different values of α	17
Figure 4.4 Maximum deflection for different values of α	18
Figure 4.5 Maximum deflection for different values of α	18
Figure 4.6 Maximum deflection for different values of α	19
Figure 4.7 Distribution of deflection along the finite difference grid.....	19
Figure 4.8 Distribution of deflection along the finite difference grid.....	20
Figure 4.9 Distribution of deflection along the finite difference grid.....	20
Figure 4.10 Distribution of deflection along the finite difference grid.....	21
Figure 4.11 Distribution of bending moment along the finite difference grid.....	21
Figure 4.12 Distribution of bending moment along the finite difference grid.....	22
Figure 4.13 Distribution of bending moment along the finite difference grid.....	22
Figure 4.14 Distribution of bending moment along the finite difference grid.....	23
Figure 4.15 Distribution of normal force along the finite difference grid	23
Figure 4.16 Distribution of normal force along the finite difference grid	24
Figure 4.17 Distribution of normal force along the finite difference grid	24
Figure 4.18 Distribution of normal force along the finite difference grid	25
Figure A.1 Maximum deflection for different values of α	35
Figure A.2 Maximum deflection for different values of α	36
Figure A.3 Maximum deflection for different values of α	36
Figure A.4 Maximum deflection for different values of α	37
Figure A.5 Distribution of deflection along the finite difference grid.....	37
Figure A.6 Distribution of deflection along the finite difference grid.....	38
Figure A.7 Distribution of deflection along the finite difference grid.....	38
Figure A.8 Distribution of deflection along the finite difference grid.....	39
Figure A.9 Distribution of bending moment along the finite difference grid.....	39
Figure A.10 Distribution of bending moment along the finite difference grid.....	40
Figure A.11 Distribution of bending moment along the finite difference grid.....	40

Figure A.12 Distribution of bending moment along the finite difference grid.....41
Figure A.13 Distribution of normal force along the finite difference grid41
Figure A.14 Distribution of normal force along the finite difference grid42
Figure A.15 Distribution of normal force along the finite difference grid42
Figure A.16 Distribution of normal force along the finite difference grid43



LIST OF TABLES

Table 2.1 Boundary Conditions	8
Table 4.1 Types of material	10
Table 4.2 W_{max} of an annular plate ($MI, y=50, Q = 1e-7$)	10
Table 4.3 W_{max} of a solid plate ($MI, y=50, Q = 1e-7$)	10
Table 4.4 Convergence study for the nondimensional maximum deflection W_{max} for a circular plate ($\alpha=0, y=100, Q=2e-8, MI$)	11
Table 4.5 Convergence study and validation of the nondimensional maximum deflection W_{max} for C-F plate ($\nu = 0.30, \kappa = 0.86, y = 1000, \alpha = 0.1$)	11
Table 4.6 Convergence study for the nondimensional maximum deflection W_{max} for annular plate ($\alpha=0.4, y=50, K_W=1, Q = (2/210) \times 10^{-5}, MI$)	12
Table 4.7 Q_6 of an annular plate ($y=50, W_{max} = 0.8, K_W = K_P = K_{NW} = 0$)	14
Table 4.8 Q_6 of an annular plate ($y=50, W_{max} = 0.8, K_W = 1, K_P = K_{NW} = 0$) ..	14
Table 4.9 Q_6 of an annular plate ($y=50, W_{max} = 0.8, K_W = 1, K_P = 1, K_{NW} = 0$)	14
Table 4.10 Q_6 of an annular plate ($y=50, W_{max} = 0.8, K_W = 1, K_P = 0, K_{NW} = 1$)	14
Table 4.11 Q_6 of an annular plate ($y=50, W_{max} = 0.8, K_W = K_P = K_{NW} = 0$)	14
Table 4.12 Q_6 of an annular plate ($y=50, W_{max} = 0.8, K_W = 1, K_P = K_{NW} = 0$) ..	15
Table 4.13 Q_6 of an annular plate ($y=50, W_{max} = 0.8, K_W = 1, K_P = 1, K_{NW} = 0$)	15
Table 4.14 Q_6 of an annular plate ($y=50, W_{max} = 0.8, K_W = 1, K_P = 0, K_{NW} = 1$)	15
Table 4.15 Q_6 of an annular plate ($y=50, W_{71} = 0.2, K_W = K_P = K_{NW} = 0$)	15
Table 4.16 Q_6 of an annular plate ($y=50, W_{71} = 0.2, K_W = 1, K_P = K_{NW} = 0$) ..	15
Table 4.17 Q_6 of an annular plate ($y=50, W_{71} = 0.2, K_W = 1, K_P = 1, K_{NW} = 0$)	15
Table 4.18 Q_6 of an annular plate ($y=50, W_{71}, K_W = 1, K_P = 0, K_{NW} = 1$)	16
Table 4.19 Q_6 of an annular plate ($y=50, W_{71} = 0.2, K_W = K_P = K_{NW} = 0$)	16
Table 4.20 Q_6 of an annular plate ($y=50, W_{71} = 0.2, K_W = 1, K_P = K_{NW} = 0$) ..	16

Table 4.21 Q_6 of an annular plate ($y=50$, $W_{71} = 0.2$, $K_W = 1$, $K_P = 1$, $K_{NW} = 0$)

..... 16

Table 4.22 Q_6 of an annular plate ($y=50$, $W_{71} = 0.2$, $K_W = 1$, $K_P = 0$, $K_{NW} = 1$)

..... 16



Axisymmetric Bending Analysis of Annular Plates

Bensu ÇÖL

Department of Civil Engineering

Mechanics Program

Master of Science Thesis

Supervisor: Prof. Dr. Murat ALTEKİN

In engineering, soil-structure interaction is a widely used research topic. Numerous elastic foundation models have been enhanced since the numerical modelling of the problem is complicated. In this study, geometrically nonlinear axisymmetric bending analysis of an orthotropic annular plate on elastic foundation is examined. The plate thickness is assumed as uniform. The formulation is based on the First Order Shear Deformation Theory. Finite Difference Method is used to solve the differential equations together with Newton-Raphson method. Deflections and stress resultants are estimated at each point in the finite difference grid. The influence of elastic foundation parameters and material properties on deflection and on stress resultants is emphasized by several numerical simulations. The results indicate that deflections and stress resultants are responsive to material properties.

Keywords: Plate, annular, nonlinear, bending, elastic foundation

Dönel Simetrik Boşluklu Plakların Eğilme Analizi

Bensu ÇÖL

İnşaat Mühendisliği Bölümü

Yüksek Lisans Tezi

Danışman: Prof. Dr. Murat ALTEKİN

Mühendislik alanında yapı-zemin etkileşimi yaygın olarak kullanılan bir araştırma konusudur. Problemin karmaşık bir sayısal modele sahip olmasından ötürü çok sayıda elastik temel modeli geliştirilmiştir. Bu çalışmada, elastik zemin üzerine oturan ortotropik dairesel bir plağın geometrik olarak doğrusal olmayan dönel simetrik eğilme analizi incelenmiştir. Plak kalınlığının sabit olduğu varsayımı yapılmıştır. Formülasyon, Birinci Dereceden Kayma Deformasyon Teorisi'ne dayanmaktadır. Diferansiyel denklem çözümlerinde Sonlu Farklar Yöntemi ile birlikte Newton-Raphson Yöntemi kullanılmıştır. Çökme ve gerilme değişkenleri sonlu fark ağındaki her noktada hesaplanmıştır. Elastik zemin parametrelerinin ve malzeme özelliklerinin sehim ve gerilme bileşkeleri üzerindeki etkisi, çeşitli sayısal simülasyonlarla vurgulanmıştır. Sonuçlar, çökme ve gerilme değişkenlerinin malzeme özelliklerine duyarlı olduğunu göstermektedir.

Anahtar Kelimeler: Plak, Boşluk, Doğrusal Olmayan, Eğilme, Elastik Zemin

1

INTRODUCTION

Numerous studies on soil-structure interaction have been carried out regarding bending behavior of circular plates. The scope of this study is limited to the geometrically nonlinear axisymmetric bending behavior of shear deformable annular plates with uniform thickness. The effect of cylindrical orthotropy is considered in the formulation. A three-parameter elastic foundation model involving Winkler, Pasternak and nonlinear Winkler is used in the analysis. The effect of several parameters on the deflection and on the stress resultants is investigated numerically.

The deformations are generally limited in engineering codes in order to prevent failure or collapse in structures. Two types of numerical simulations are made in the study. First, the deformations are determined for a given external load. Next, the unknowns including the external load are computed for a given deflection. The second approach may be helpful to have an insight on the load carrying capacity of the plate.

1.1 Literature Review

Plate analysis is a commonly used research topic in engineering. Vibration, bending and buckling analysis are generally processed for plate analysis.

Nath and Jain [1] presented nonlinear transient analyses of orthotropic annular shallow shells resting on elastic foundation. Dumir and Shingal [2] investigated bending behavior of thick cylindrically orthotropic circular plates. Chen and Hwang [3] examined vibration analyses of thick annular plates using FEM. Salehi and Turvey [4] studied large deflection analyses of annular plates using DR method combined with FDM. Vibration analyses of thick, polar orthotropic annular plates with variable thicknesses are presented by Soamidas and Ganesan [5]. Smaill [6] analyzed large deflection axisymmetric bending of cylindrically orthotropic thin annular plates on Pasternak foundations. Han and Liew [7] examined axisymmetric bending analyses of moderately thick circular plates by using DQM. Han and Liew [8] studied axisymmetric bending analyses of moderately thick annular plates under static loading using DQM.

Axisymmetric bending analyses of FGM circular and annular plates using Mindlin plate theory are examined by Reddy, Wang, and Kitipornchai [9]. Utku, Çıtıptıoğlu, İnceleme [10] carried out bending analyses of annular plates on elastic foundation. Liu and Lee [11] studied vibration analysis of thick circular and annular plates using FEM. Vibration analyses of Reissner plates resting on Pasternak foundation are investigated by Eratlı and Aköz [12] using FEM. Nie and Zhong [13] presented axisymmetric bending analyses of FGM circular and annular plates using methods of SSM and DQM. Nonlinear bending analyses of FGM square plates using CPT studied by Alinia and Ghannadpour [14]. Civalek and Ersoy [15] presented free vibration and bending analyses of thick circular plates using Singular Convolution Method. Artan and Lehmann [16] studied bending analyses of nonlocal elastic annular plates using Initial Values Method. Yahnioglu and Yesil [17] carried out the vibration analyses of thick rectangular composite plates with a circular hole using FEM. Yalçın, Arıkoğlu, Özkol [18] examined vibration analyses of circular thin plates using DTM. Tekin and Coskun [19] investigated the dynamic response of circular plates on two-parameter tensionless elastic foundation. Sharma [20] investigated axisymmetric vibration analyses of orthotropic annular plates resting on Pasternak foundation. Golmakani and Kadkhodayan [21] examined nonlinear bending analyses of annular FGM plates using DR theory combined with FDM. Akgoz and Civalek [22] presented geometrically nonlinear vibration analyses of thin laminated plates resting on nonlinear elastic foundations. Kutlu, Arıbaş, Karayığit, Omurtag [23] presented the bending analysis of Mindlin elliptic plates resting on arbitrarily orthotropic elastic foundation. Altekin [24] investigated geometrically nonlinear bending analyses of axisymmetric annular plates under transverse loading. Kutlu and Omurtag [25] studied large deflection bending analyses of moderately thick elliptic plates using FEM. Rad and Shariyat [26] examined bending analyses of FGM annular plates resting on non-uniform two-parameter Winkler-Pasternak foundation using DQM. Large deflection analyses of FGM annular plates resting on two-parameter elastic foundations using DR method combined with FDM investigated by Golmakani and Alamatian [27]. Hamad, Tarlochan [28] studied axisymmetric bending analyses of FGM annular plates using generalized DQM. Roknuzzaman, Hossain, Haque, Ahmed [29] examined bending analyses of thin rectangular plate with opening using FDM.

Mercan [30] studied axisymmetric bending analyses of circular plates with variable thickness using FDM. Yılmaz [31] presented bending analysis of rectangular and circular plates using FDM. Nonlinear bending analyses of spherical shallow shells and circular plates using FDM are examined by Gökdağ [32]. Altekin [33] carried out bending analyses of super-elliptical Mindlin plates using FEM. Large deflection analyses of thin annular plates using FEM are performed by Kömürçü, Demirkan, Yılmaz [34]. Karapınar [35] studied buckling analyses of elliptical FGM plates with variable thickness under thermal loads. Noori [36] investigated axisymmetric bending and vibration analyses of circular plates with FGM. Khare and Mittal [37] examined free vibration analyses of symmetrically laminated circular and annular plates with elastic edge constraints using DQM. Draiche et. al. [38] studied statical analyses of laminated reinforced composite plates using FSDT. Belardi et. al. [39] studied bending analyses of shear deformable rectilinear orthotropic composite annular plates. Altekin [40, 41] investigated nonlinear bending analyses of circular plates with orthotropy resting on elastic foundation, and large deflection bending analyses of circular plates using FDM and DQM with combined effects of material properties. Buckling analyses of rectangular orthotropic composite thick plates are studied by Karataş [42] by using 3D FEM. Plaut [43] examined large deflection analyses of thin circular and annular plates using Reissner theory. Kutlu and Omurtag [44] studied buckling analyses of rectangular moderately thick plates on orthotropic foundation. Noori and Temel [45] examined vibration analyses thick annular plates with variable thickness. Axisymmetric bending analyses of functionally graded FSDT annular plates with variable thickness are carried out by Noori and Temel [46]. Fundamental frequencies of annular elliptical FSDT plates using FEM are investigated by Altekin [47]. Köme [48] studied bending analyses of Mindlin plates resting on 4-parameter elastic foundation using DTM. Yüce [49] investigated bending analyses of thin circular plates using DTM. Gao, Pang, Li, Jia, Tang [50] studied vibration analysis of circular and annular plates using FEM and Rayleigh-Ritz Method. Bending, buckling and vibration analyses of FGM circular and annular plates using DQM are presented by Wei and Qing [51]. Vasara et. al. [52] examined free vibration analyses of porous FGM annular plates using DQM. Kim et. al. [53] studied nonlinear axisymmetric bending analyses of FGM porous annular plates using FEM.

1.2 Objective of the Thesis

The objective of the thesis is to observe the soil-structure interaction of annular plates by means of Winkler, Pasternak, and nonlinear Winkler elastic foundation models. Vertical displacements and stress resultants of annular plates with isotropic and orthotropic material properties are presented. Numerical simulation is carried out by geometrically nonlinear analysis. Numerical results are compared by use of Ansys software.

1.3 Hypothesis

Geometrically nonlinear bending analysis of an axisymmetric annular plate on 3-parameter elastic foundation with cylindrical orthotropy and uniform thickness is the contribution of this study. Formulations are based on FSDT, and solution method is FDM. The soil-structure interaction through elastic foundation, and the effect of material through isotropy and orthotropy are observed.

2.1 Formulation

Among several shear deformation theories, due to its simplicity in implementation the First Order Shear Deformation Theory (FSDT) is preferred in this study. Cylindrical orthotropy is included in the formulation [1,2] which involves geometrical nonlinearity.

The thickness of the plate is uniform. The circular cutout is concentric with the plate which is subjected to a uniformly distributed transverse pressure (Fig. 2.1).

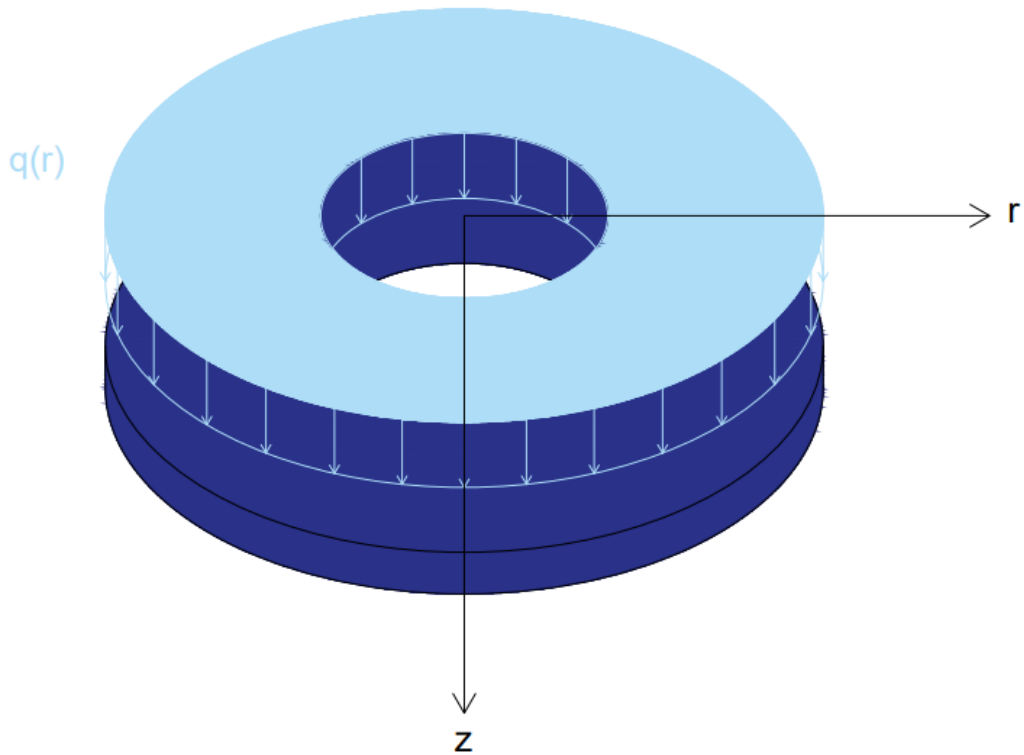


Figure 2.1 Annular plate under transverse loading

The geometry of the plate is defined by the parameters y and α introduced by

$$y = \frac{a}{h} \quad (2.1)$$

$$\alpha = \frac{b}{a} \quad 0 \leq \alpha < 1 \quad (2.2)$$

As a special case, the solution of a solid plate can be obtained for $\alpha=0$. Annular plates are introduced by two-letter symbols [8]. For instance, F-C means an annular plate with a free (F) inner edge, and a clamped (C) outer edge [8]. Likewise, S-C indicates an annular plate with a simply supported (S) inner edge, and a clamped (C) outer edge [8]. Solid plates are shown by one-letter symbols such as S or C. For example, S means a simply supported (S) plate. The elastic foundation is characterized by a three-parameter model.

2.2 Variables and Governing Equations

The governing equations of an axisymmetric plate are given by [1],[2]

$$(rn_r)' - n_\theta = 0 \quad (2.3)$$

$$(rm_r)' - m_\theta - rq_r = 0 \quad (2.4)$$

$$(rw'n_r + rq_r)' + r\left(q - k_W w + k_P w'' + \frac{k_p}{r} w' - k_{NW} w^3\right) = 0 \quad (2.5)$$

where $()' = d()/dr$.

Relations between stress resultants and deformations of a cylindrically orthotropic plate are given by [2]

$$n_r = \frac{E_\theta h}{(\lambda - \nu_\theta^2)} \left(u' + \frac{1}{2} (w')^2 + \nu_\theta \frac{u}{r} \right) \quad (2.6)$$

$$n_\theta = \frac{E_\theta h}{(\lambda - \nu_\theta^2)} \left(\nu_\theta u' + \frac{\nu_\theta}{2} (w')^2 + \lambda \frac{u}{r} \right) \quad (2.7)$$

$$m_r = D \left(\psi' + \nu_\theta \frac{\psi}{r} \right) \quad (2.8)$$

$$m_\theta = D \left(\nu_\theta \psi' + \lambda \frac{\psi}{r} \right) \quad (2.9)$$

$$q_r = \kappa h G_{rz} (\psi + w') \quad (2.10)$$

where

$$\lambda = \frac{\nu_\theta}{\nu_r} = \frac{E_\theta}{E_r} \quad (2.11)$$

$$D = \frac{E_\theta h^3}{12(\lambda - \nu_\theta^2)} \quad (2.12)$$

The non-dimensional variables and parameters are introduced by

$$w = Wh \quad , \quad u = Uh \quad (2.13)$$

$$m_r = M_r E_\theta h^2 \quad , \quad m_\theta = M_\theta E_\theta h^2 \quad (2.14)$$

$$n_r = N_r E_\theta h \quad , \quad n_\theta = N_\theta E_\theta h \quad (2.15)$$

$$q_r = Q_r E_\theta h \quad , \quad q = Q E_\theta \quad (2.16)$$

$$k_w = \frac{E_\theta h^3}{a^4} K_w \quad , \quad k_p = \frac{E_\theta h^3}{a^2} K_p \quad , \quad k_{NW} = \frac{E_\theta h}{a^4} K_{NW} \quad (2.17)$$

Upon substituting Eqs. (2.11-2.17) into Eqs. (2.3-2.5)

$$\begin{aligned} & y(\lambda - v_\theta^2)(1 - \alpha)N_r + y(\lambda - v_\theta^2)Y \frac{dN_r}{dX} - v_\theta \frac{dU}{dX} - \frac{v_\theta}{2y(1 - \alpha)} \left(\frac{dW}{dX} \right)^2 \\ & - \lambda \frac{(1 - \alpha)}{Y} U = 0 \end{aligned} \quad (2.18)$$

$$\begin{aligned} & y(\lambda - v_\theta^2)M_r + \frac{y(\lambda - v_\theta^2)}{(1 - \alpha)} Y \frac{dM_r}{dX} - \frac{v_\theta}{12(1 - \alpha)} \frac{d\psi}{dX} - \frac{\lambda}{12Y} \psi \\ & - y^2(\lambda - v_\theta^2)YQ_r = 0 \end{aligned} \quad (2.19)$$

$$\begin{aligned} & \frac{dW}{dX} N_r + \frac{Y}{(1 - \alpha)} \frac{dW}{dX} \frac{dN_r}{dX} + \frac{y\lambda}{\kappa\eta} Y N_r \frac{dQ_r}{dX} - yY \frac{d\psi}{dX} N_r + y(1 - \alpha)Q_r + yY \frac{dQ_r}{dX} \\ & + y^2 Y (1 - \alpha) Q - K_w \frac{(1 - \alpha)}{y^2} YW + \frac{\lambda K_p}{y\kappa\eta} Y \frac{dQ_r}{dX} - \frac{K_p}{y} Y \frac{d\psi}{dX} + \frac{K_p}{y^2} \frac{dW}{dX} \\ & - \frac{(1 - \alpha)}{y^2} Y K_{NW} W^3 = 0 \end{aligned} \quad (2.20)$$

are obtained where [1]

$$r = R + b \quad 0 \leq r \leq a \quad (2.21)$$

$$Y = \frac{R + b}{a} \quad (2.22)$$

$$R = (a - b)X \quad 0 \leq X \leq 1 \quad (2.23)$$

The material properties are defined by the parameters λ and η where [2]

$$\eta = \frac{G_{rz}}{E_r} \quad (2.24)$$

2.3 Boundary Conditions

The boundary conditions shown in Table 2.1 are satisfied exactly at the inner and outer edges of the annular plate. Likewise, the regularity conditions given by

$$u = \psi = q_r = 0 \quad (2.25)$$

at the center of a solid plate are satisfied exactly.

Table 2.1 Boundary Conditions

	Boundary Conditions
C	$w=0, u=0, \Psi=0$
S	$w=0, u=0, m_r=0$
F	$n_r=0, q_r=0, m_r=0$

The system of differential equations in the current study forms a boundary value problem which is solved numerically by means of FDM together with Newton-Raphson method.

3.1 Finite Difference Method

Finite Difference Method is one of the widely used conventional discretization methods in applied mathematics. FDM makes it possible to transform a differential equation into a system of algebraic equations using a grid in the problem domain (Fig. 3.1). Forward, and backward difference formulations are given by [54].

$$f'_i \cong \frac{-3f_i + 4f_{i+1} - f_{i+2}}{2\Delta} \quad , \quad f'_i \cong \frac{f_{i-2} - 4f_{i-1} + 3f_i}{2\Delta} \quad (3.1)$$

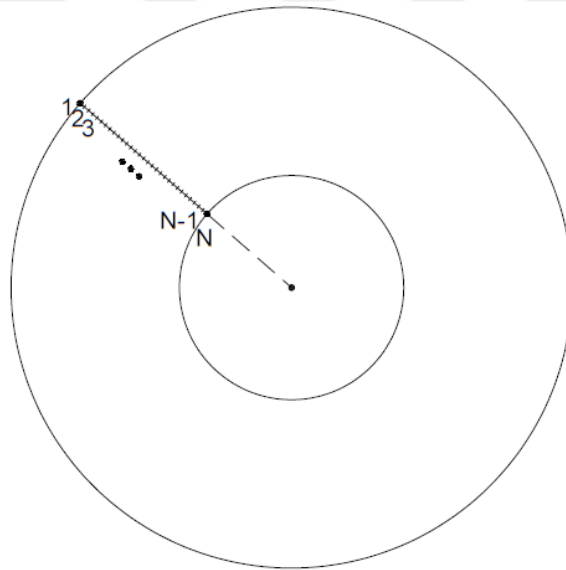


Figure 3.1 FDM grid

3.2 Newton-Raphson Method

The system of nonlinear algebraic equations is solved by means of the Newton-Raphson Method, which is one of the frequently employed iterative solution methods in literature.

4.1 Convergence Study and Validation of Results

Unless otherwise stated (i) $\kappa=5/6$, and (ii) the material properties shown in Table 4.1 are used in the analysis. The numerical solutions reveal that a satisfactory rate of convergence is achieved for $N=141$ (Tables 4.2-4.4). Reliability of the numerical simulations in this dissertation is checked via comparison studies including ANSYS solutions (Tables 4.4-4.6, Figures 4.1-4.2). Some of the figures which may be helpful to understand the bending behavior of the plate are shown in Appendix.

Table 4.1 Types of material

Type of Material	Abbreviation	Material Properties
Isotropic	MI	$\nu_0 = 0.30$, $\lambda = 1$
Orthotropic [2]	MO	$\nu_0 = 0.25$, $\lambda = 10$, $\eta = 0.4$

Table 4.2 W_{max} of an annular plate (MI, $y=50$, $Q = 1e-7$)

$\alpha=0.2$	N=101 (L)	N=121 (L)	N=141 (L)		N=101 (NL)	N=121 (NL)	N=141 (NL)
F-S	0.507897	0.508059	0.508157		0.392497	0.392594	0.392654
F-C	0.109636	0.109659	0.109673		0.108959	0.108982	0.108996
S-F	0.817938	0.818077	0.818164		0.643277	0.643326	0.43357
S-S	0.030935	0.030933	0.030934		0.030865	0.030863	0.030864
S-C	0.012546	0.012548	0.012549		0.012544	0.012545	0.012546
C-F	0.353374	0.353208	0.353109		0.341742	0.341594	0.341505
C-S	0.016978	0.016976	0.016974		0.016971	0.016968	0.016967
C-C	0.00751	0.007511	0.007511		0.00751	0.00751	0.007511

Table 4.3 W_{max} of a solid plate (MI, $y=50$, $Q = 1e-7$)

$\alpha=0$	N=101 (L)	N=121 (L)	N=141 (L)		N=101 (NL)	N=121 (NL)	N=141 (NL)
S	0.434905	0.434922	0.434932		0.351574	0.351583	0.351588
C	0.106801	0.106812	0.106818		0.106147	0.106158	0.106164

Table 4.4 Convergence study for the nondimensional maximum deflection W_{max} for a circular plate ($\alpha=0$, $y=100$, $Q=2e-8$, MI)

Edge of the plate	W_{max}	Type of solution	
(S)	1.3914	(L)	N = 401 [32]
(S)	1.3911	(L)	N = 81
(S)	1.3912	(L)	N = 91
(S)	1.3912	(L)	N = 101
(S)	1.3913	(L)	N = 141
(C)	0.3414	(L)	N = 401 [32]
(C)	0.3412	(L)	N = 81
(C)	0.3413	(L)	N = 91
(C)	0.3413	(L)	N = 101
(C)	0.3413	(L)	N = 141
(S)	0.7037	(NL)	N = 401 [32]
(S)	0.7037	(NL)	N = 81
(S)	0.7037	(NL)	N = 91
(S)	0.7037	(NL)	N = 101
(S)	0.7037	(NL)	N = 141
(C)	0.3230	(NL)	N = 401 [32]
(C)	0.3228	(NL)	N = 81
(C)	0.3228	(NL)	N = 91
(C)	0.3229	(NL)	N = 101
(C)	0.3229	(NL)	N = 141

Table 4.5 Convergence study and validation of the nondimensional maximum deflection W_{max} for C-F plate ($\nu = 0.30$, $\kappa = 0.86$, $y = 1000$, $\alpha = 0.1$)

(L)	W_{max}
N = 81	0.7606×10^{-1}
N = 91	0.7598×10^{-1}
N = 101	0.7593×10^{-1}
[7]	0.75693×10^{-1}

Table 4.6 Convergence study for the nondimensional maximum deflection W_{max}
for annular plate ($\alpha=0.4$, $y=50$, $K_w=1$, $Q = (2/210) \times 10^{-5}$, MI)

MI	ANSYS (L)	FDM (L) N=91		ANSYS (NL)	FDM (NL) N=91
Boundary conditions (inner-outer)	W_{max}	W_{max}		W_{max}	W_{max}
C-C	0.00223	0.0022		0.00223	0.0022
C-S	0.00489	0.0049		0.00489	0.0049
C-F	0.10086	0.1011		0.10069	0.1010
S-C	0.00416	0.0042		0.00416	0.0042
S-S	0.01034	0.0103		0,01034	0.0103
F-C	0.05577	0.0559		0.05571	0.0558

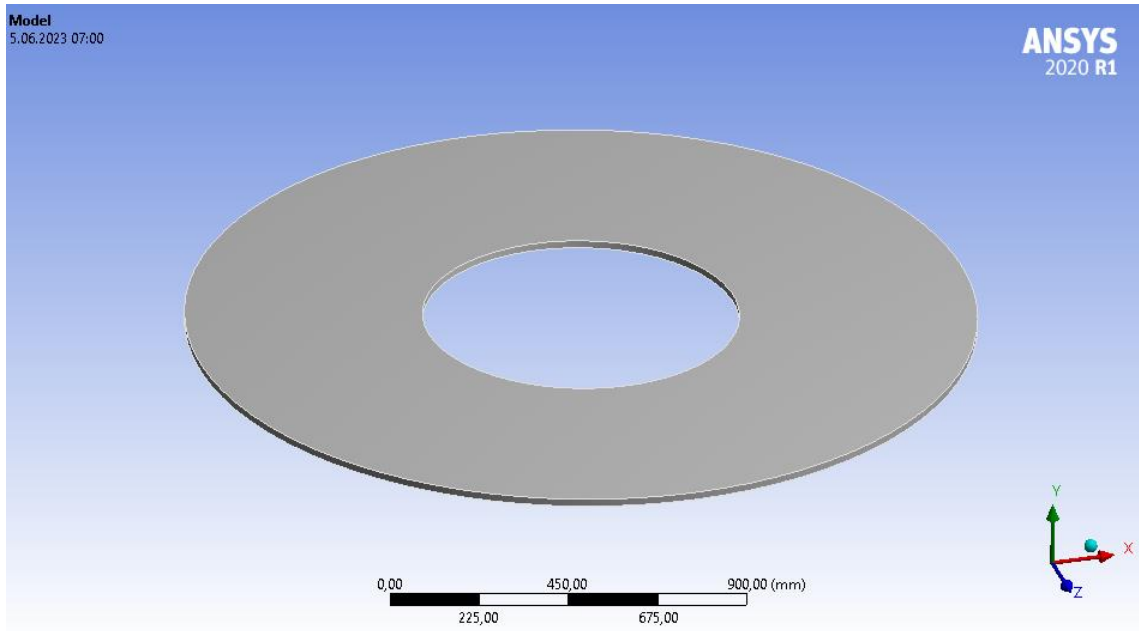


Figure 4.1 Model of the annular plate (ANSYS)

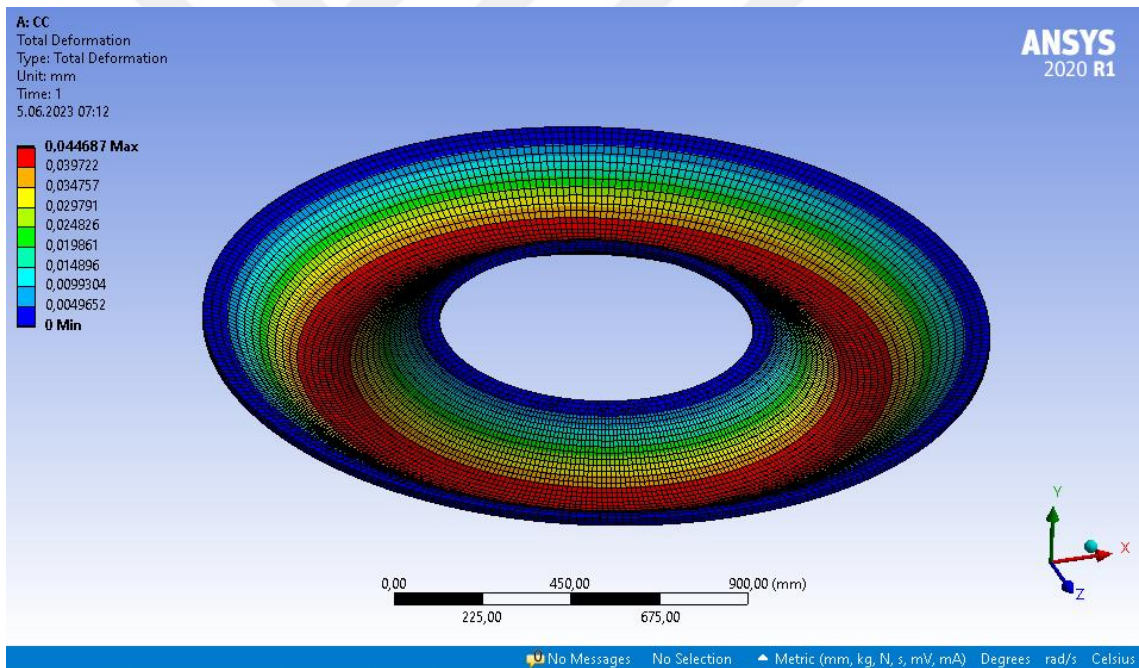


Figure 4.2 Deformed form of the annular C-C plate (ANSYS)

4.2 Numerical Examples

A large number of examples are solved to make a comprehensive analysis. First, for a given external load ($Q=1e-7$), the problem is solved (Figures 4.3-4.18). Next, for a given nodal displacement ($W_{max} = 0.8$), the external load Q_6 where $Q_6 = Q \times 10^6$ is found (Tables 4.7-4.14). Finally, for a given nodal displacement ($W_{71} = 0.2$), where W_{71} denotes the nondimensional deflection at node 71, the external load Q_6 is calculated (Tables 4.15-4.22). Unless otherwise reported $N = 141$ is used in the calculations.

Table 4.7 Q_6 of an annular plate ($y=50$, $W_{max} = 0.8$, $K_W = K_P = K_{NW} = 0$)

MI, (NL)	$\alpha=0.2$	$\alpha=0.4$	$\alpha=0.6$
F-S	0.358162	0.386623	0.579441
F-C	0.9761	1.569947	5.158444

Table 4.8 Q_6 of an annular plate ($y=50$, $W_{max} = 0.8$, $K_W = 1$, $K_P = K_{NW} = 0$)

MI, (NL)	$\alpha=0.2$	$\alpha=0.4$	$\alpha=0.6$
F-S	0.44162	0.467809	0.661226
F-C	1.05529	1.648942	5.239023

Table 4.9 Q_6 of an annular plate ($y=50$, $W_{max} = 0.8$, $K_W = 1$, $K_P = 1$, $K_{NW} = 0$)

MI, (NL)	$\alpha=0.2$	$\alpha=0.4$	$\alpha=0.6$
F-S	0.864037	0.83161	1.038041
F-C	1.485769	1.931291	5.340297

Table 4.10 Q_6 of an annular plate ($y=50$, $W_{max} = 0.8$, $K_W = 1$, $K_P = 0$, $K_{NW} = 1$)

MI, (NL)	$\alpha=0.2$	$\alpha=0.4$	$\alpha=0.6$
F-S	0.473159	0.497466	0.691307
F-C	1.083869	1.677515	5.268781

Table 4.11 Q_6 of an annular plate ($y=50$, $W_{max} = 0.8$, $K_W = K_P = K_{NW} = 0$)

MO, (NL)	$\alpha=0.2$	$\alpha=0.4$	$\alpha=0.6$
F-S	0.16862	0.233045	0.440853
F-C	0.296989	0.441359	1.036664

Table 4.12 Q_6 of an annular plate ($y=50$, $W_{max} = 0.8$, $K_W = 1$, $K_P = K_{NW} = 0$)

MO, (NL)	$\alpha=0.2$	$\alpha=0.4$	$\alpha=0.6$
F-S	0.268906	0.328602	0.53067
F-C	0.392948	0.53199	1.122449

Table 4.13 Q_6 of an annular plate ($y=50$, $W_{max} = 0.8$, $K_W = 1$, $K_P = 1$, $K_{NW} = 0$)

MO, (NL)	$\alpha=0.2$	$\alpha=0.4$	$\alpha=0.6$
F-S	0.840962	0.943637	1.215715
F-C	1.00597	1.158053	1.673465

Table 4.14 Q_6 of an annular plate ($y=50$, $W_{max} = 0.8$, $K_W = 1$, $K_P = 0$, $K_{NW} = 1$)

MO, (NL)	$\alpha=0.2$	$\alpha=0.4$	$\alpha=0.6$
F-S	0.319102	0.372197	0.567576
F-C	0.438468	0.570839	1.156284

Table 4.15 Q_6 of an annular plate ($y=50$, $W_{71} = 0.2$, $K_W = K_P = K_{NW} = 0$)

MI, (NL)	$\alpha=0.2$	$\alpha=0.4$	$\alpha=0.6$
S-S	0.711573	2.029449	9.930431
C-C	2.764662	8.751029	43.68563

Table 4.16 Q_6 of an annular plate ($y=50$, $W_{71} = 0.2$, $K_W = 1$, $K_P = K_{NW} = 0$)

MI, (NL)	$\alpha=0.2$	$\alpha=0.4$	$\alpha=0.6$
S-S	0.73698	2.054837	9.955812
C-C	2.789696	8.775961	43.71054

Table 4.17 Q_6 of an annular plate ($y=50$, $W_{71} = 0.2$, $K_W = 1$, $K_P = 1$, $K_{NW} = 0$)

MI, (NL)	$\alpha=0.2$	$\alpha=0.4$	$\alpha=0.6$
S-S	1.115393	2.741104	11.51393
C-C	3.250837	9.612239	45.59763

Table 4.18 Q_6 of an annular plate ($y=50$, W_{71} , $K_W = 1$, $K_P = 0$, $K_{NW} = 1$)

MI, (NL)	$\alpha=0.2$	$\alpha=0.4$	$\alpha=0.6$
S-S	0.737755	2.055609	9.956582
C-C	2.79046	8.776714	43.71129

Table 4.19 Q_6 of an annular plate ($y=50$, $W_{71} = 0.2$, $K_W = K_P = K_{NW} = 0$)

MO, (NL)	$\alpha=0.2$	$\alpha=0.4$	$\alpha=0.6$
S-S	0.175291	0.309381	1.104403
C-C	0.378694	0.943203	4.236207

Table 4.20 Q_6 of an annular plate ($y=50$, $W_{71} = 0.2$, $K_W = 1$, $K_P = K_{NW} = 0$)

MO, (NL)	$\alpha=0.2$	$\alpha=0.4$	$\alpha=0.6$
S-S	0.201119	0.334883	1.129821
C-C	0.40387	0.968219	4.261149

Table 4.21 Q_6 of an annular plate ($y=50$, $W_{71} = 0.2$, $K_W = 1$, $K_P = 1$, $K_{NW} = 0$)

MO, (NL)	$\alpha=0.2$	$\alpha=0.4$	$\alpha=0.6$
S-S	0.596918	1.03039	2.696608
C-C	0.857421	1.792977	6.135921

Table 4.22 Q_6 of an annular plate ($y=50$, $W_{71} = 0.2$, $K_W = 1$, $K_P = 0$, $K_{NW} = 1$)

MO, (NL)	$\alpha=0.2$	$\alpha=0.4$	$\alpha=0.6$
S-S	0.201922	0.335661	1.130593
C-C	0.404636	0.968975	4.2619

4.3 Numerical Results

Numerical simulations are carried out for geometrically nonlinear bending analysis of annular plates. Deflections and stress resultants are observed for MI and MO plates on elastic foundation.

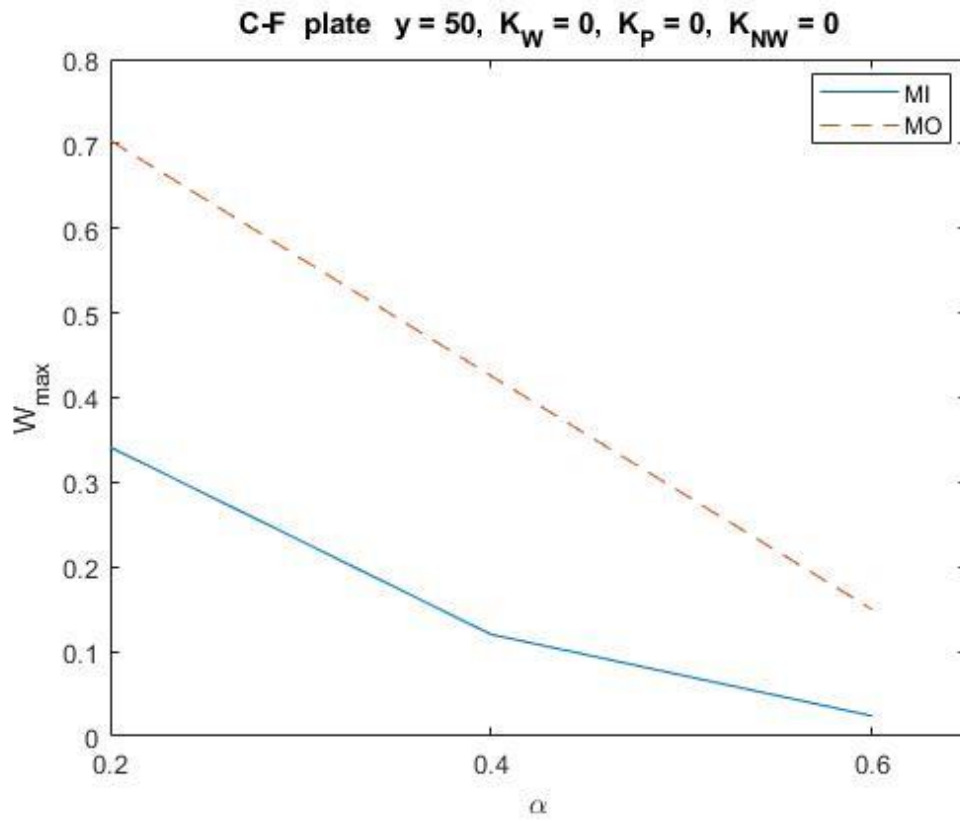


Figure 4.3 Maximum deflection for different values of α

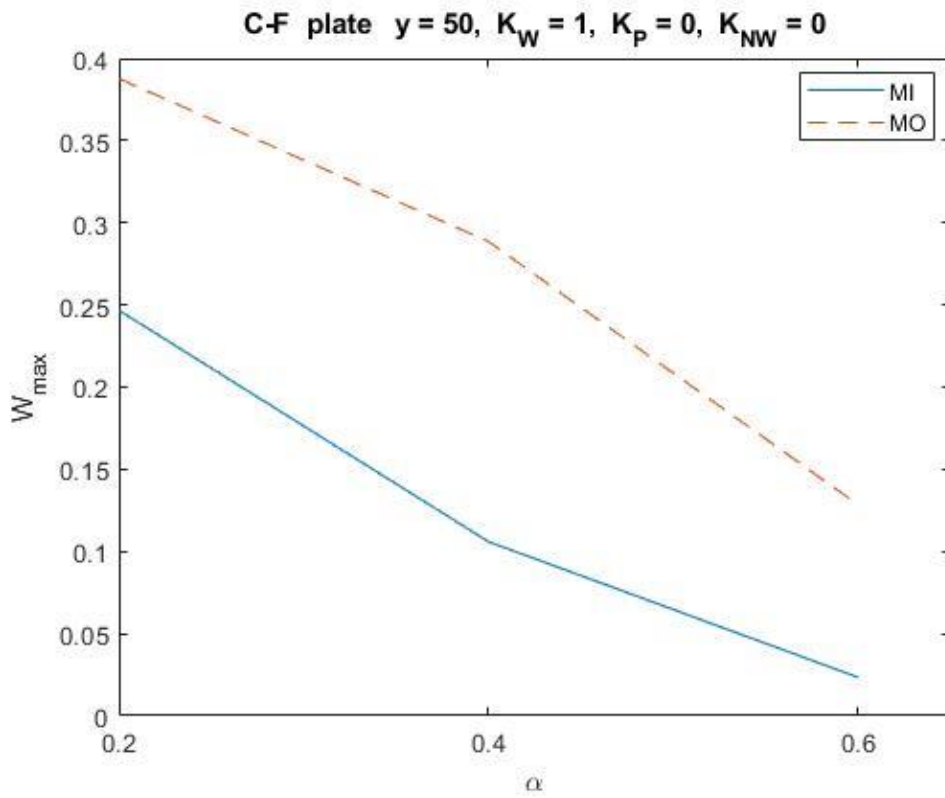


Figure 4.4 Maximum deflection for different values of α

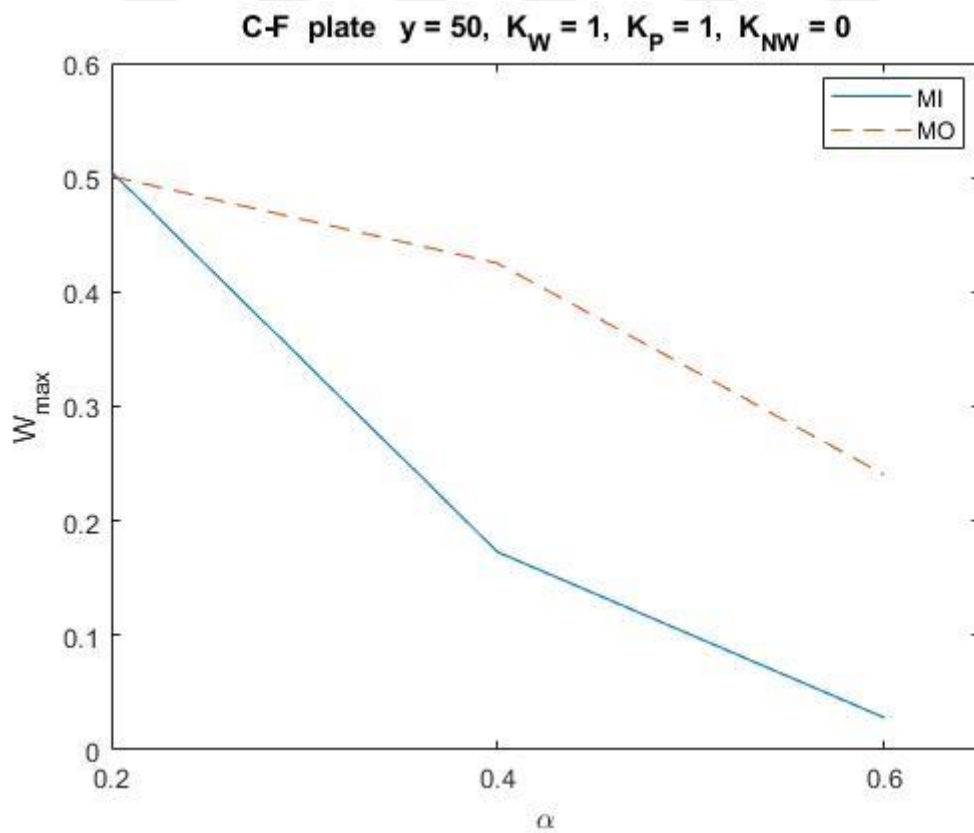


Figure 4.5 Maximum deflection for different values of α

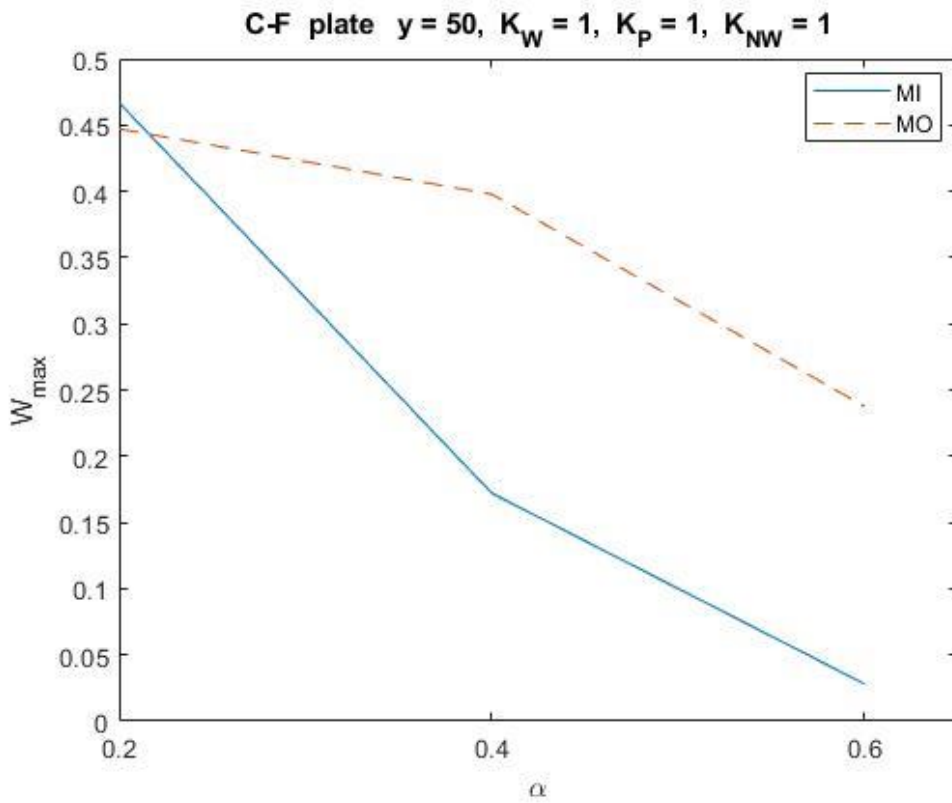


Figure 4.6 Maximum deflection for different values of α

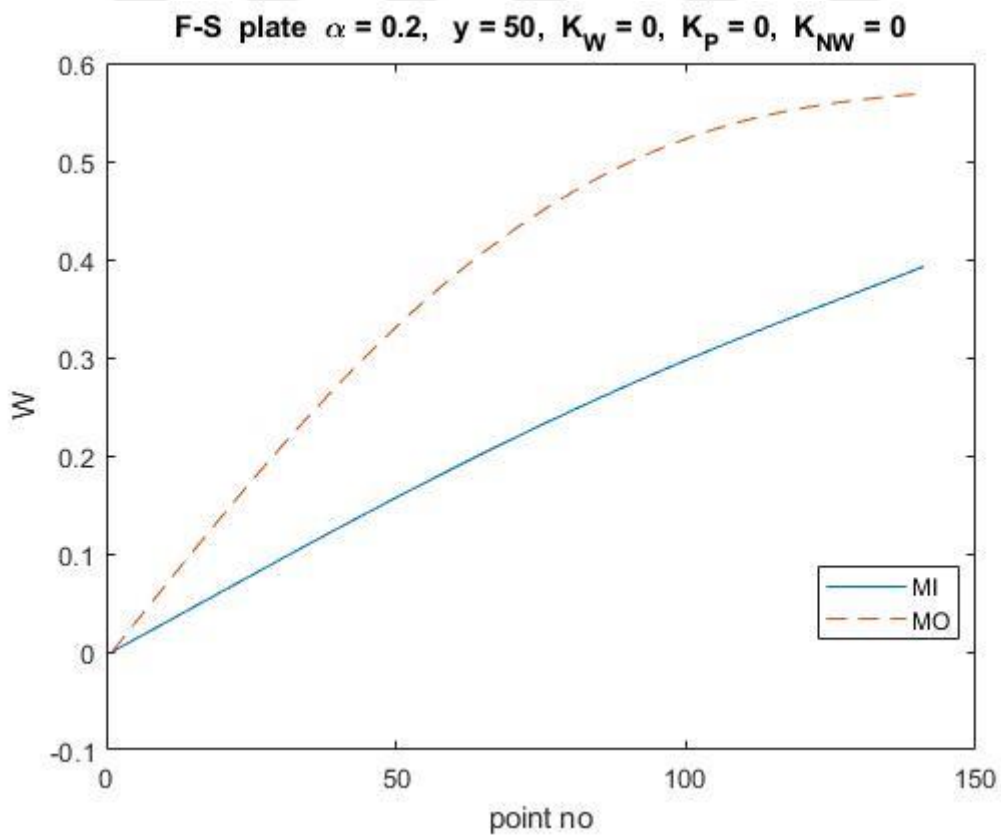


Figure 4.7 Distribution of deflection along the finite difference grid

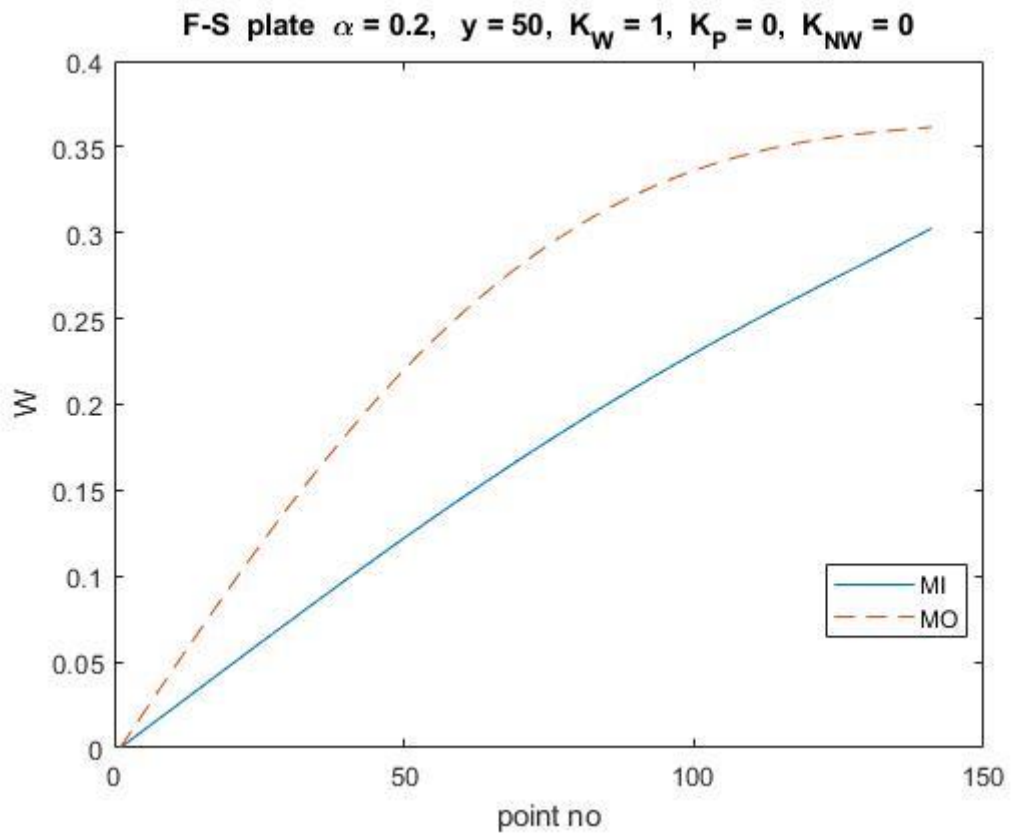


Figure 4.8 Distribution of deflection along the finite difference grid

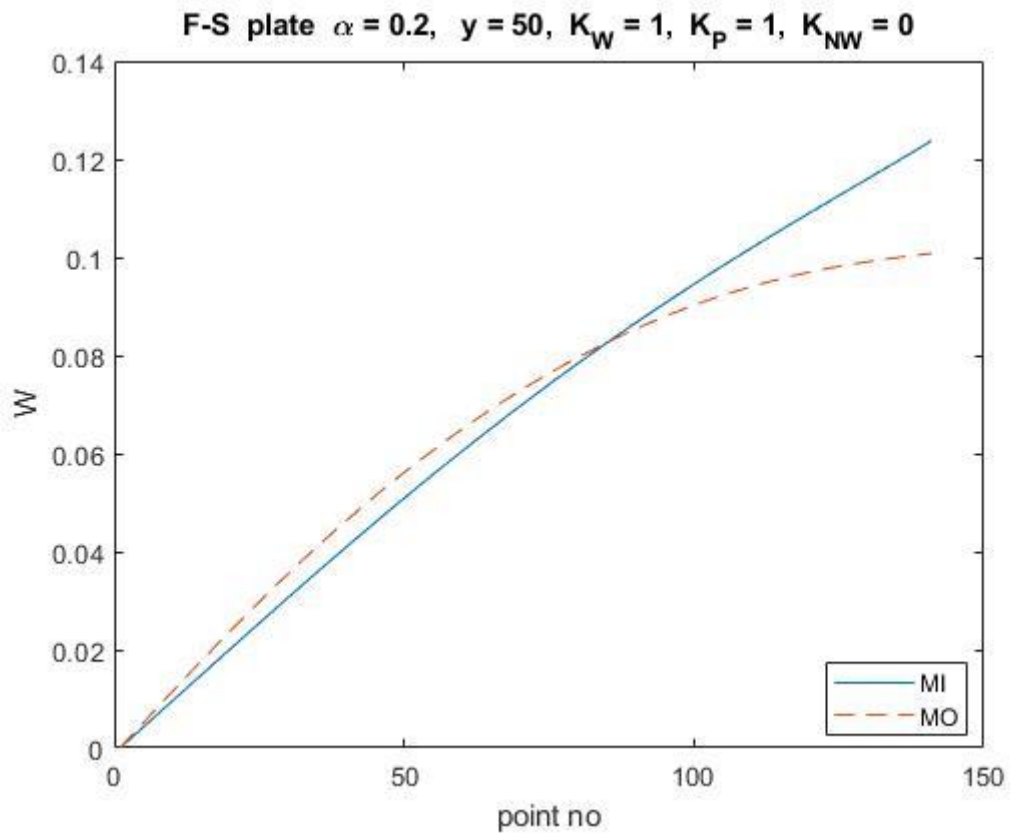


Figure 4.9 Distribution of deflection along the finite difference grid

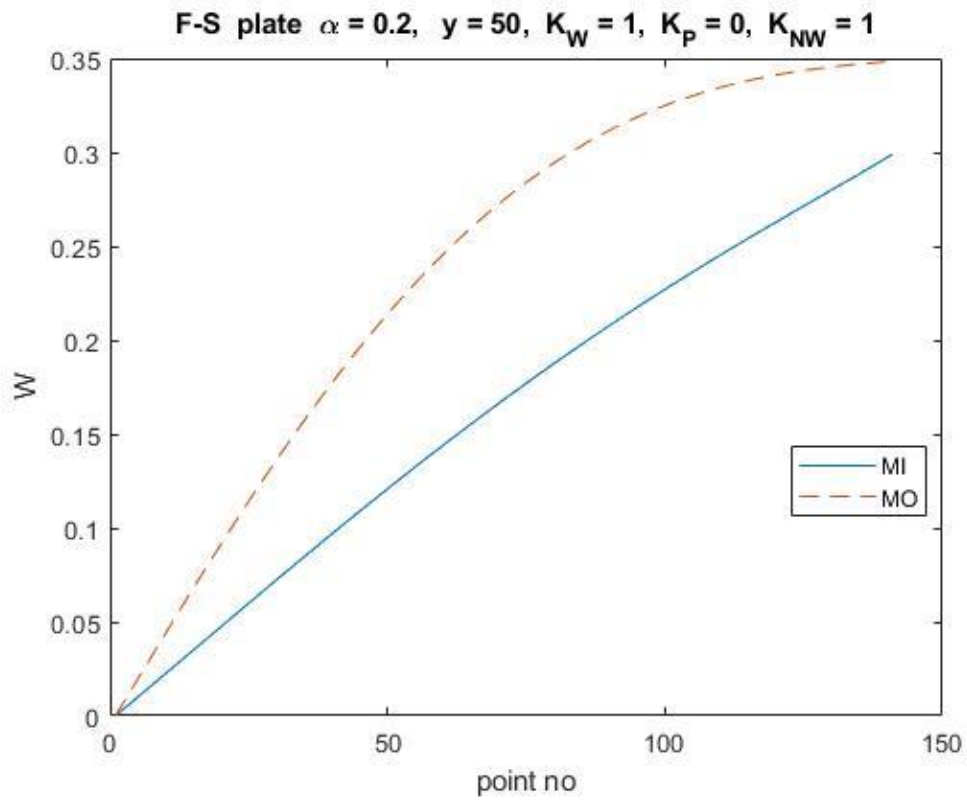


Figure 4.10 Distribution of deflection along the finite difference grid

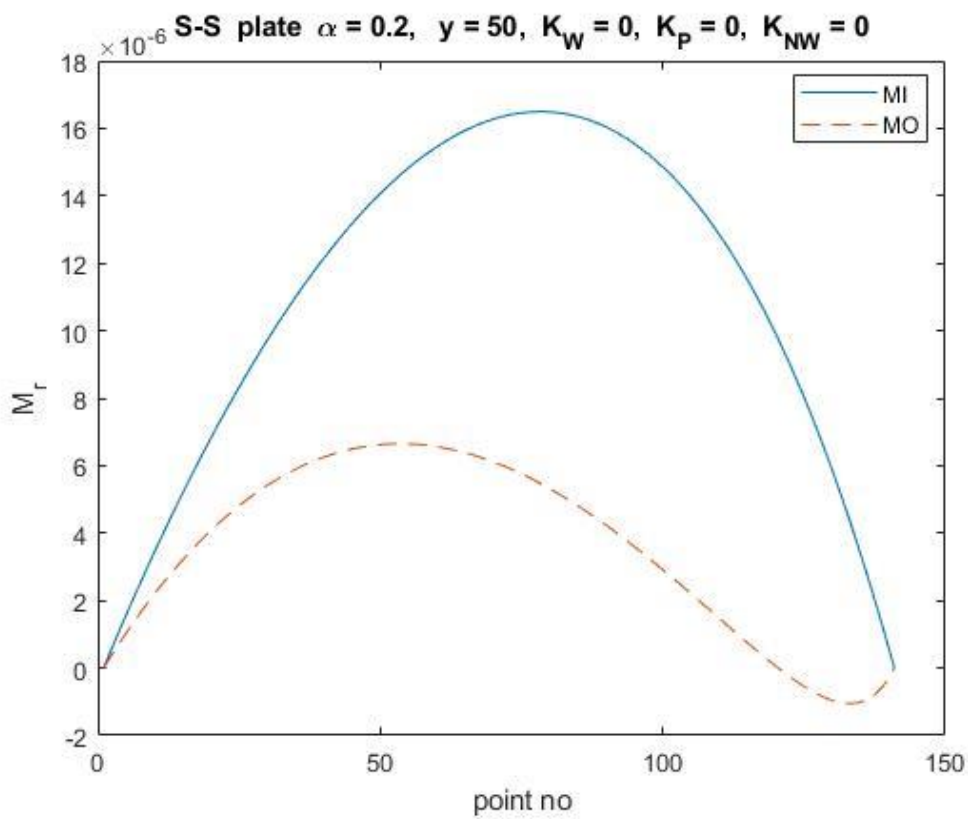


Figure 4.11 Distribution of bending moment along the finite difference grid

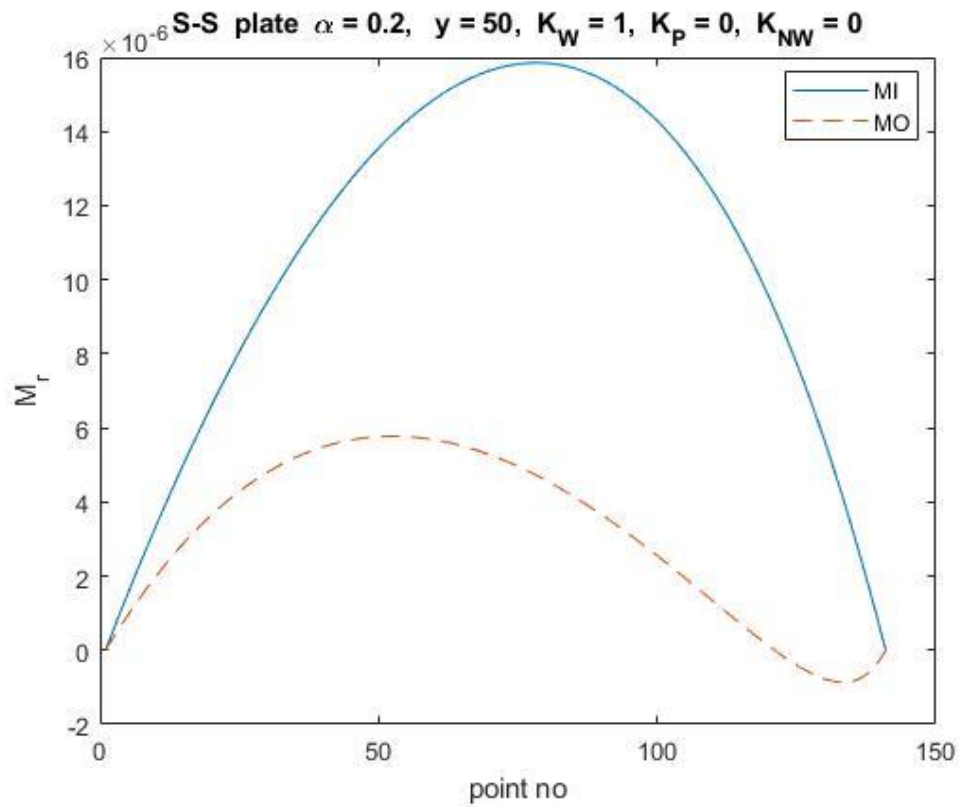


Figure 4.12 Distribution of bending moment along the finite difference grid

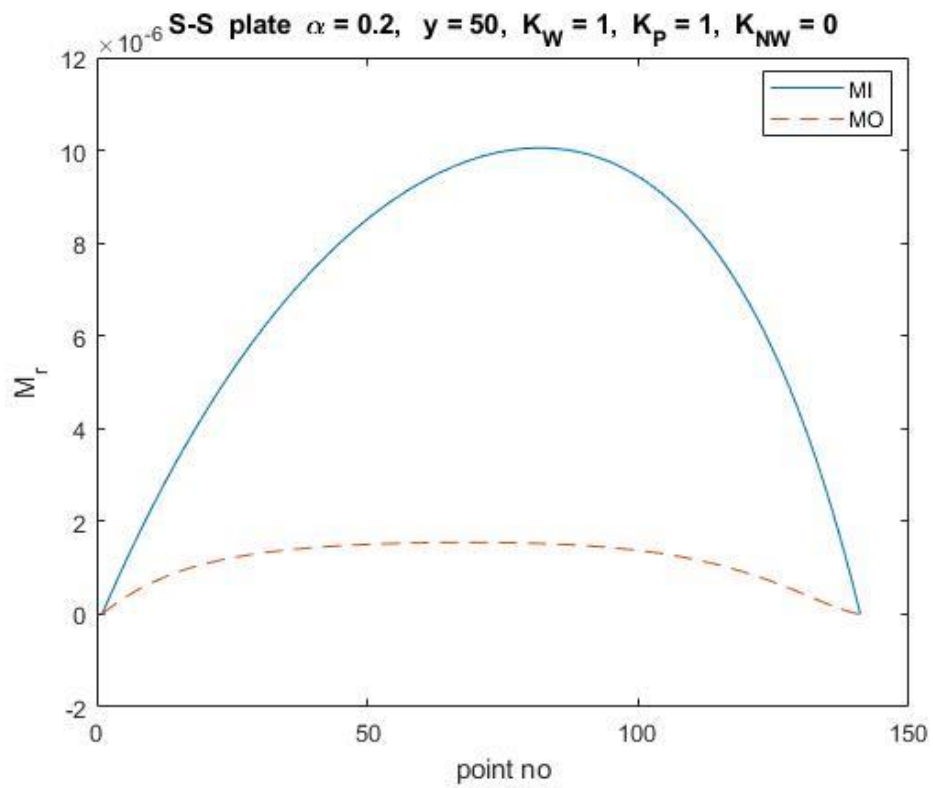


Figure 4.13 Distribution of bending moment along the finite difference grid

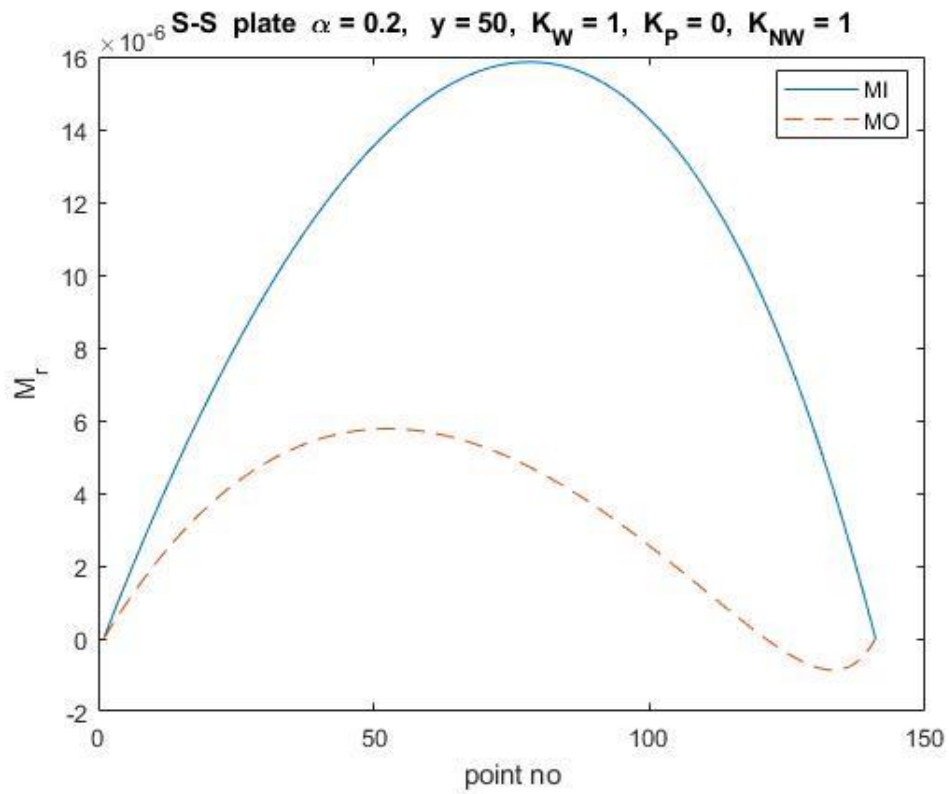


Figure 4.14 Distribution of bending moment along the finite difference grid

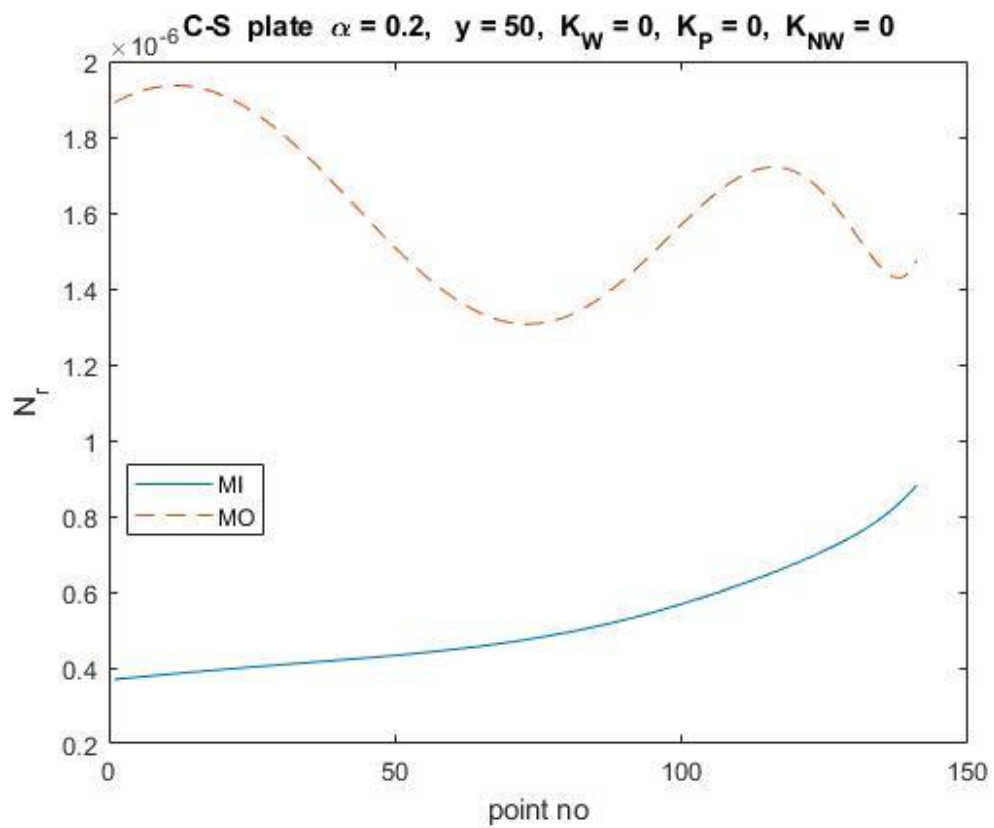


Figure 4.15 Distribution of normal force along the finite difference grid

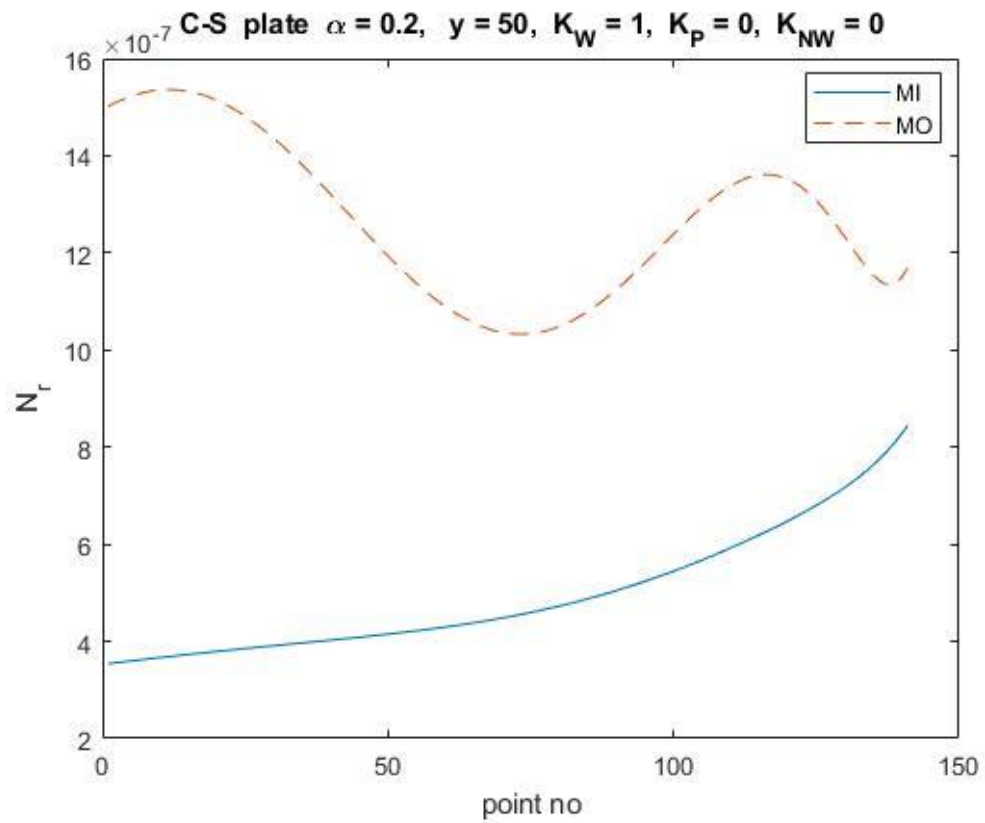


Figure 4.16 Distribution of normal force along the finite difference grid

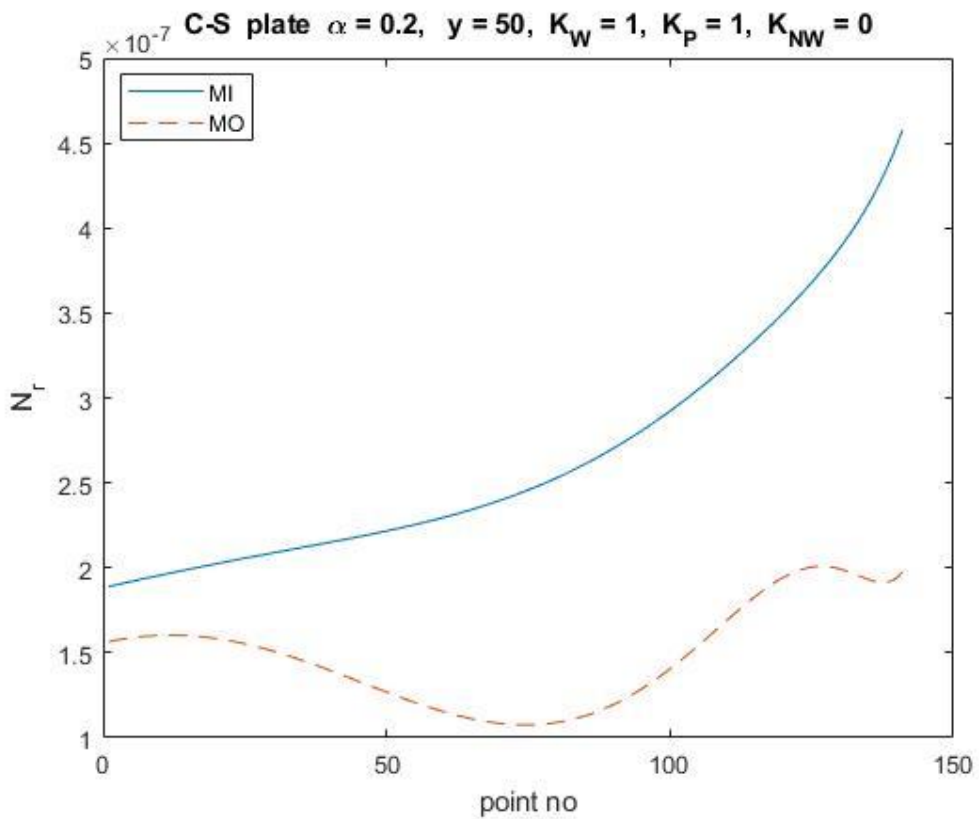


Figure 4.17 Distribution of normal force along the finite difference grid

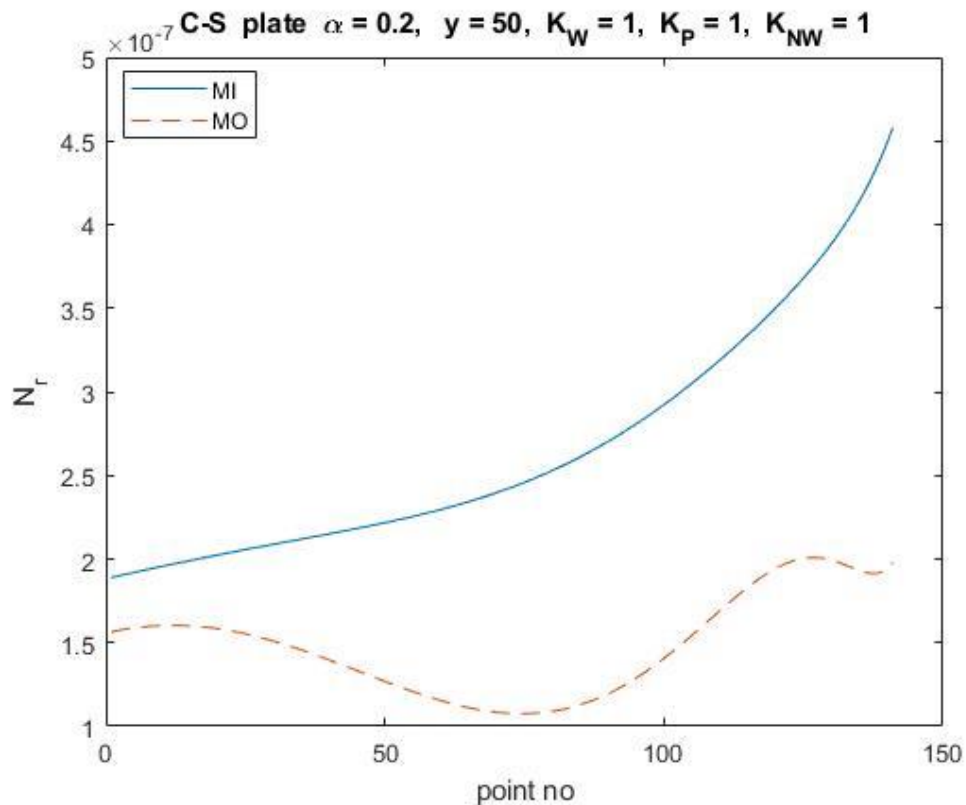


Figure 4.18 Distribution of normal force along the finite difference grid

The effects of plate geometry, material properties, boundary conditions, and elastic foundation are emphasized for deflection and stress resultants.

- Geometrical nonlinearity has a significant effect on the reduction of the maximum deflection (Tables 4.2-4.4, Table 4.6).
- Boundary conditions have a major influence on deflections. By contribution of the clamped edges, maximum deflections are minimized (Tables 4.2-4.4, Table 4.6).
- The analysis also covers a displacement control approach. $W_{max} = 0.8$ is chosen since it is a quite high deflection which can be considered sufficient to observe the effect of nonlinearity (Tables 4.7-4.14).
 - With a constant maximum deflection, as α increases, the transverse loading increase (Tables 4.7-4.22).
- Compared to F-S plate, the load carrying capacity of F-C plate is higher (Tables 4.7-4.14).
 - C-C plate has higher load values than S-S plate for a constant maximum deflection (Tables 4.15-4.22).

- The effect of Winkler parameter increases the loading (Table 4.8, Table 4.12, Table 4.16, Table 4.20).
- Pasternak parameter increases the loading (Table 4.9, Table 4.13, Table 4.17, Table 4.21).
- If there is NL Winkler parameter, loading increases (Table 4.10, Table 4.14, Table 4.18, Table 4.22).
- The elastic foundations increases the load capacity of the annular plate (Tables 4.7-4.22).
- MO plate loading is lower than MI plate loading for a constant maximum deflection due to designated material parameters (Tables 4.7-4.22).
- For C-F plate,
 - As α increases, maximum deflection decreases (Figs. 4.3-4.6).
 - The combined effect of Winkler, Pasternak, and NL Winkler elastic foundation parameters minimize the maximum deflection (Figs. 4.4-4.6).
- For F-S plate,
 - Maximum deflections develop at the inner edge (F) (Figs. 4.7-4.10).
 - MI causes greater results on maximum deflections rather than MO for assigned material parameters (Figs. 4.7-4.10).
 - In the presence of Winkler elastic foundation parameter, maximum deflection declines (Fig. 4.8).
 - Influence of Pasternak elastic foundation causes maximum deflection to decrease significantly (Fig. 4.9).
 - Influence of Nonlinear Winkler elastic foundation leads to the reduction of maximum deflection (Fig. 4.10).
- For S-S plate,
 - The maximum moment of MI plate is observed in the vicinity of the center of grid points (Figs. 4.11-4.14).
 - MI plate has higher moments than MO plate (Figs. 4.11-4.14).
 - Moments decrease by the definition of Winkler, Pasternak and NL Winkler parameters (Figs. 4.12-4.14).

- For C-S plate,
 - Since the analysis type is geometrically nonlinear, the distribution of the normal force is shown (Figs. 4.15-4.18).
 - Normal force in MI plate increases from outer edge to inner edge with a more linear behavior, while normal force in MO plate varies (Figs. 4.15-4.18).
 - When Winkler parameter is included, normal forces decrease (Fig. 4.16).
 - MI plate has lower normal force values than MO plate. However, when MO plate is on Pasternak foundation, there is a remarkable decline for normal force values (Fig. 4.17).
 - With the presence of Pasternak and NL Winkler parameters, MI plate has higher normal force values than MO plate (Fig. 4.18).

5

CONCLUSION

In this study, axisymmetric bending behavior of annular plates with uniform thickness under uniform transverse pressure is observed. Geometrical nonlinearity is included in the formulation which is based on FSDT. The solution is obtained by means of FDM together with Newton-Raphson method. The effects of material properties are examined with conditions of isotropy and cylindrical orthotropy. Soil-structure interaction is observed using Winkler, Pasternak and nonlinear Winkler elastic foundation models. Various combinations for the boundary conditions are investigated in the numerical examples.

Numerical studies have been performed to examine the effects of (i) the size of the cutout (i.e., the inner radius the plate), (ii) the material properties, (iii) the elastic foundation parameters, and (iv) the boundary conditions on the deflection and on the stress resultants.

Increase in the size of the cutout, with a given deflection, maximize the load carrying capacity of annular plates. For a given loading, it minimizes the maximum deflections. The load carrying capacity or the maximum deflections are affected by the material parameters. The presence of one-parameter, two-parameter or three-parameter elastic foundations decreases the maximum deflections and the stress resultants. With a given deflection, they increase the load carrying capacity of the plate. Boundary conditions have a significant effect on plate deflections and stress resultants. Clamped edges increase the load carrying capacity of the annular plate with a given displacement.

REFERENCES

- [1] Y. Nath and R. K. Jain ,“Orthotropic Annular Shells on Elastic Foundations”, *J. Eng. Mech.*, vol. 111, pp. 1242-1256, 1985, doi: 10.1061/(ASCE)0733-9399(1985)111:10(1242) .
- [2] P.C Dumir and L. Shingal, “Nonlinear Analysis of Thick Circular Plates”, *J. Eng. Mech.*, vol.112, no.3, pp. 260-272, 1986, doi: 10.1061/(ASCE)0733-9399(1986)112:3(260) .
- [3] L.W. Chen and J.R. Hwang, “Finite Element Analysis of Thick Annular Plates Under Internal Forces”, *Computers & Structures*, vol. 32, no. 1, pp. 63-68, 1989, doi: 10.1016/0045-7949(89)90069-2 .
- [4] M. Salehi and G. J. Turvey, “Elastic Large Deflection Response of Annular Sector Plates-A Comparison of DR Finite-Difference, Finite Element and Other Numerical Solutions”, *Computers & Structures*, vol. 40, no.5, pp. 1267-1278, 1991, doi: 10.1016/0045-7949(91)90397-5.
- [5] V. Soamidas and N. Ganesan, “Vibration Analysis of Thick, Polar Orthotropic, Variable Thickness Annular Disks”, *Journal of Sound and Vibration*, vol.147, no. 1, pp. 39-56, 1991, doi: 10.1016/0022-460X(91)90682-A .
- [6] J.S Smaill, “Large Deflection Response of Annular Plates on Pasternak Foundations”, *Int. J. Solid Structures*, vol. 27. no. 8. pp.1073-1084, 1991.
- [7] J.B. Han, K. M. Liew, “Analysis of Moderately Thick Circular Plates Using Differential Quadrature Method”, *Journal of Engineering Mechanics*, vol. 123, no.12, pp. 1247-1252, 1997, doi: 10.1061/(ASCE)0733-9399(1997)123:12(1247).
- [8] J.B. Han and K. M. Liew, “Analysis of Annular Reissner/Mindlin Plates Using Differential Quadrate Method”, *Int. J. Mech. Sci.*, vol. 40, no. 7, pp. 651-661, 1998, doi: 10.1016/S0020-7403(97)00087-8.
- [9] J.N. Reddy, C.M. Wang, S. Kitipornchai, “Axisymmetric Bending of Functionally Graded Circular and Annular Plates”, *Eur. J. Mech. A/Solids*, vol.18, pp.185-199, 1999, doi: 10.1016/S0997-7538(99)80011-4.
- [10] M. Utku, E. Çıtıptıoğlu, İ. İnceleme, “Circular Plates on Elastic Foundations Modelled with Annular Plates”, *Computers and Structures*, vol. 78, pp.365-374, 2000, doi :10.1016/S0045-7949(00)00063-8.

- [11] C.F Liu, Y.T Lee, “Finite Element Analysis of Three-Dimensional Vibrations of Thick Circular and Annular Plates”, *Journal of Sound and Vibration*, vol.233, no. 1, pp. 63-80, 2000, doi: 10.1006/jsvi.1997.1228.
- [12] N. Eratlı, A. Y. Aköz, “Free Vibration Analysis of Reissner Plates by Mixed Finite Element”, *Structural Engineering and Mechanics*, vol. 13, no. 3, pp.277-298, 2002, doi: 10.1006/jsvi.1997.1228.
- [13] G. Nie, Z. Zhong, “Axisymmetric Bending of Two-Directional Functionally Graded Circular and Annular Plates”, *Acta Mechanica Solida Sinica*, vol. 20, no. 4, 2007, doi: 10.1007/s10338-007-0734-9.
- [14] M.M. Alinia, S.A.M. Ghannadpour, “Nonlinear Analysis of Pressure Loaded FGM Plates”, *Composite Structures*, vol.88, pp. 354–359, 2009, doi: 10.1016/j.compstruct.2008.04.013.
- [15] Ö. Civalek, H. Ersoy, “Free Vibration and Bending Analysis of Circular Mindlin Plates Using Singular Convolution Method”, *Communications in Numerical Methods in Engineering*, vol.25, pp. 907-922, 2009, doi: 10.1002/cnm.1138
- [16] R. Artan, L. Lehmann, “Initial Values Method for Symmetric Bending of Micro/Nano Annular Circular Plates Based on Nonlocal Plate Theory”, *Journal of Computational and Theoretical Nanoscience*, vol. 6, no. 5, pp. 1125-1130, 2009, doi: 10.1166/jctn.2009.1153.
- [17] N. Yahnioglu, U. B. Yesil, “Forced Vibration of an Initial Stressed Rectangular Composite Thick Plate with a Cylindrical Hole”, ASME International Mechanical Engineering Congress and Exposition, Lake Buena Vista, Florida, USA, November 13–19, 2009, pp.337-343, doi: 10.1115/IMECE2009-10475.
- [18] H.S. Yalçın, A. Arıkoğlu, İ. Özkol , “Free Vibration Analysis of Circular Plates by Differential Transformation Method”, *Applied Mathematics and Computation*, vol 212, no. 2, pp. 377-386, 2009, doi: 10.1016/j.amc.2009.02.032.
- [19] A Tekin, I Coskun, “Dynamic Response of a Circular Plate Resting on a Tensionless Vlasov Foundation”, SEMC2010, Cape-Town, South Africa, September 6-8, 2010, pp.565-568.

- [20] S. Sharma, U.S. Gupta and R.Lal, "Effect of Pasternak Foundation on Axisymmetric Vibration of Polar Orthotropic Annular Plates of Varying Thickness", *Journal of Vibration and Acoustics*, vol. 132, no.4, pp. 1-13, 2010, doi: 10.1115/1.4001495.
- [21] M.E. Golmakani and M. Kadkhodayan, "Nonlinear Bending Analysis of Annular FGM Plates Using Higher-Order Shear Deformation Plate Theories", *Composite Structures*, vol.93, pp. 973–982, 2011, doi: 10.1016/j.compstruct.2010.06.024.
- [22] B. Akgoz, O. Civalek, "Nonlinear Vibration Analysis of Laminated Plates Resting on Nonlinear Two-Parameters Elastic Foundations", *Steel and Composite Structures*, vol. 11, no: 5, pp. 403-421, 2011, doi: 10.12989/scs.2011.11.5.403.
- [23] A Kutlu, Ü.N. Aribaş, H. Karayiğit, M.H. Omurtag, "Flexure of the Moderately Thick Elliptic Plates on Arbitrarily Orthotropic Elastic Foundation", International Symposium on Advances in Applied Mechanics and Modern Information Technology, Baku, Azerbaijan, September, 2011, pp. 210-214.
- [24] M. Altekin, "Axisymmetric Large Deflection Analysis of an Annular Circular Plate subject to Rotational Symmetric Loading", The Eleventh International Conference on Computational Structures Technology, January, 2012, pp. 182, [Online].
- [25] A. Kutlu and M. H. Omurtag, "Large Deflection Bending Analysis of Elliptic Plates on Orthotropic Elastic Foundation with Mixed Finite Element Method", *International Journal of Mechanical Sciences*, vol. 65, pp. 64–74, 2012, doi: 10.1016/j.ijmecsci.2012.09.004.
- [26] A.B Rad and M. Shariyat, "A Three-Dimensional Elasticity Solution for Two-Directional FGM Annular Plates with Non-Uniform Elastic Foundations Subjected to Normal and Shear Traction", *Acta Mechanica Solida Sinica*, vol. 26, no. 6, 2013, doi: 10.1016/S0894-9166(14)60010-0.
- [27] M.E. Golmakani and J. Alamatian, "Large Deflection Analysis of Shear Deformable Radially Functionally Graded Sector Plates on Two-Parameter Elastic Foundations", *European Journal of Mechanics A/Solids*, vol. 42, pp.251-265, 2013, doi: 10.1016/j.euromechsol.2013.06.006.

- [28] M.H. Hamad, F. Tarlochan, “An Axisymmetric Bending Analysis of Functionally Graded Annular Plate Under Transverse Load via Generalized Differential Quadrature Method”, *IJRET: International Journal of Research in Engineering and Technology*, 2013, eISSN: 2319-1163, pISSN: 2321-7308.
- [29] Roknuzzaman, B. Hossain, R. Haque, T.U. Ahmed, “Analysis of Rectangular Plate with Opening by Finite Difference Method”, *American Journal of Civil Engineering and Architecture*, vol. 3, no. 5, pp.165-173, 2015.
- [30] A. Mercan, “Axisymmetric Bending Analysis of a Circular Plate with Variable Thickness Under Statical Loading”, Msc Thesis, Yildiz Technical University, İstanbul, Türkiye, 2016.
- [31] A. Yılmaz, “Dairesel Plakların Sonlu Farklar ile Çözülmesi”, Msc Thesis, İstanbul Technical University, İstanbul, Türkiye, 2016.
- [32] S. Gökdağ, “Sığ Küresel Kabukların ve Dairesel Plakların Doğrusal Olmayan Eğilme Analizi”, Msc Thesis, Yildiz Technical University, İstanbul, Türkiye, 2018.
- [33] M. Altekin, "Bending of Super-Elliptical Mindlin Plates by Finite Element Method", *Teknik Dergi/Tech. J. Turkish Chamb. of Civil Eng.*, vol.29, no.4, pp. 8469-8496, 2018, doi: 10.18400/tekderg.332384.
- [34] S. Kömürcü, E. Demirkan, M. Yılmaz, “Numerical Large Deflection Analysis of Annular Plates”, 13th International Congress on Advances in Civil Engineering, İzmir, Turkey, September 12-14, 2018.
- [35] S. Karapınar, “Determination of Buckling Temperatures for Elliptical FGM Plates with Variable Thicknesses”, *Uludağ University Journal of The Faculty of Engineering*, vol. 24, no. 1, pp. 75-88, 2019, doi: 10.17482/uumfd.480661.
- [36] A.R. Noori, “Axisymmetric Bending and Flexural Vibration Analysis of Heterogeneous (FGM) Circular Plates”, PhD Thesis, Çukurova University, Adana, Türkiye, 2019.
- [37] S. Khare, N.D. Mittal, “Axisymmetric Bending and Free Vibration of Symmetrically Laminated Circular and Annular Plates Having Elastic Edge Constraints”, *Ain Shams Engineering Journal*, vol.10, pp. 343–352, 2019, doi: 10.1016/j.asej.2018.10.006.

- [38] K. Draiche, A. A. Bousahla, A. Tounsi, A. S. Alwabli, A. Tounsi and S.R. Mahmoud, “Static Analysis of Laminated Reinforced Composite Plates Using a Simple First-Order Shear Deformation Theory”, *Computers and Concrete*, vol. 24, no.4, pp. 369-378, 2019, doi: 10.12989/cac.2019.24.4.369.
- [39] V. G. Belardi, P. Fanelli, F. Vivio, “First-Order Shear Deformation Analysis of Rectilinear Orthotropic Composite Circular Plates Undergoing Transversal Loads”, *Composites Part:B Engineering*, vol.174, Art. no.:107015, 2019, doi: 10.1016/j.compositesb.2019.107015.
- [40] M. Altekin, "Axisymmetric Nonlinear Bending of Shear Deformable Orthotropic Circular Plates on Elastic Foundation", PCM-CMM 2019, Krakow, Poland, 2019.
- [41] M. Altekin, “Combined Effects of Material Properties and Boundary Conditions on the Large Deflection Bending Analysis of Circular Plates on a Nonlinear Elastic Foundation”, *Computers and Concrete*, vol. 25, no. 6, pp. 537-549, 2020, doi: 10.12989/cac.2020.25.6.537.
- [42] E. E. Karataş, “Buckling Delamination of a Rectangular Orthotropic Thick Plate with an Embedded Rectangular Crack Subjected to an Axial Compressive Force”, *Mechanics of Composite Materials*, vol. 55, pp.643–654, 2019, doi: 10.1007/s11029-019-09841-w.
- [43] R. H. Plaut, “Generalized Reissner Analysis of Large Axisymmetric Deflections of Thin Circular and Annular Plates”, *International Journal of Solids and Structures*, vol.203, pp. 131–137, 2020, doi: 10.1016/j.ijsolstr.2020.08.004.
- [44] A. Kutlu, M.H. Omurtag, “Buckling of Rectangular FSDT Plates Resting on Orthotropic Foundation by Mixed FEM”, *Sigma J Eng & Nat Sci*, vol.38, no.2, pp. 659-666, 2020.
- [45] A. R. Noori, B. Temel, “A Unified Solution for the Vibration Analysis of Two-Directional Functionally Graded Axisymmetric Mindlin-Reissner Plates with Variable Thickness”, *International Journal of Mechanical Sciences*, vol. 174, no.3, Art. no.:105471, 2020, doi: 10.1016/j.ijmecsci.2020.105471.
- [46] A. R. Noori, B. Temel, “A Powerful Numerical Approach for the Axisymmetric Bending Response of Shear Deformable Two-Directional Functionally Graded (2D-FG) Plates with Variable Thickness”, *Proceedings of the Institution of Mechanical Engineers, Part C: Journal of Mechanical*

- Engineering Science*, vol.235, no.22, pp. 1989-1996, 2021, doi: 10.1177/09544062211010837.
- [47] M. Altekin, “Fundamental Frequencies of Elliptical Plates using Static Deflections”, *Teknik Dergi*, pp.11569-11589, Paper 648, 2022, doi: 10.18400/tekderg.817251.
- [48] A. Köme, “Bending Analysis of Circular Plates”, Msc Thesis, Yıldız Technical University, İstanbul, Türkiye, 2022.
- [49] B. Yüce, “Axisymmetric Bending Analysis of Circular Plates resting on Elastic Eoundation”, Msc Thesis, Yildiz Technical University, İstanbul, Türkiye, 2022.
- [50] C. Gao, F. Pang, H. Li, D. Jia, Y. Tang, “Steady and Transient Vibration Analysis of Uniform and Stepped Annular/Circular Plates based on FSDT”, *Acta Mechanica*, vol. 233, pp. 1061-1082, 2022, doi: 10.1007/s00707-022-03157-y.
- [51] L. Wei, H. Qing, “Bending, Buckling and Vibration Analysis of Bi-Directional Functionally Graded Circular/Annular Microplate based on MCST”, *Composite Structures*, vol. 292, Art. no.: 115633, 2022, doi: 10.1016/j.compstruct.2022.115633.
- [52] D. Vasara, S. Khare, H. K. Sharma, R. Kumar, “Free Vibration Analysis of Functionally Graded Porous Circular and Annular Plates Using Differential Quadrature Method”, *Forces in Mechanics*, vol.9, Art. no.: 100126, 2022, doi: 10.1016/j.finmec.2022.100126.
- [53] J. Kim, E. Nava, S. Rakici, “Nonlinear Finite Element Model for Bending Analysis of Functionally-Graded Porous Circular/Annular Micro-Plates under Thermomechanical Loads Using Quasi-3D Reddy Third-Order Plate Theory”, *Computational Mechanics of Structures and Materials*, vol.16, no. 9, 3505, 2023, doi: 10.3390/ma16093505
- [54] J. H. Mathews, *Numerical Methods for Mathematics, Science and Engineering*, Vol X, Englewood Cliffs, New Jersey, USA, Prentice-Hall International, 1992, ISBN 0-13-625047-5.

ADDITIONAL NUMERICAL RESULTS

Additional numerical simulation results with different boundary conditions for better understanding of the bending behavior of the annular plate are shown in Figures A.1-A.16.

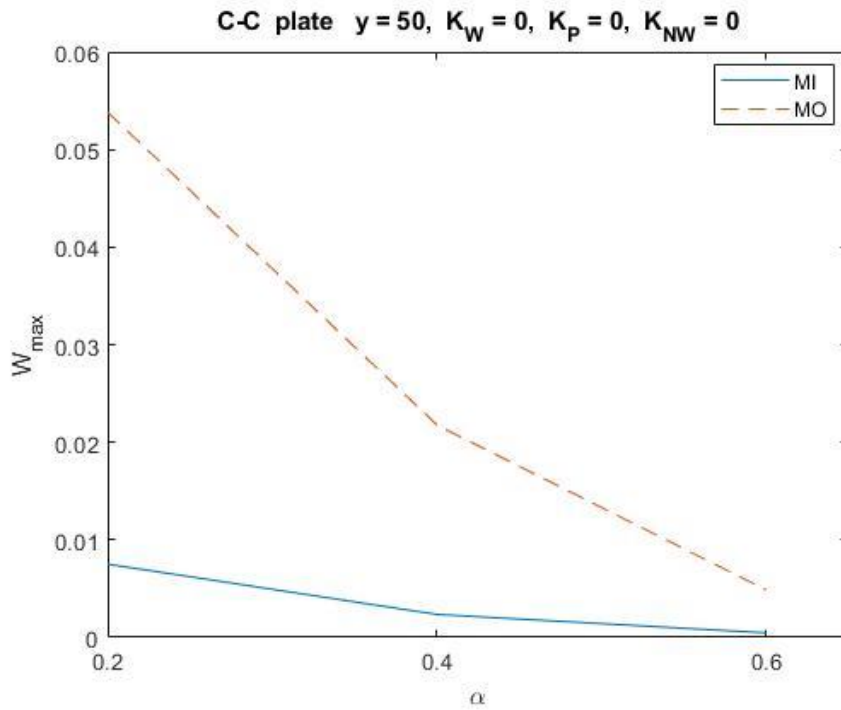


Figure A.1 Maximum deflection for different values of α

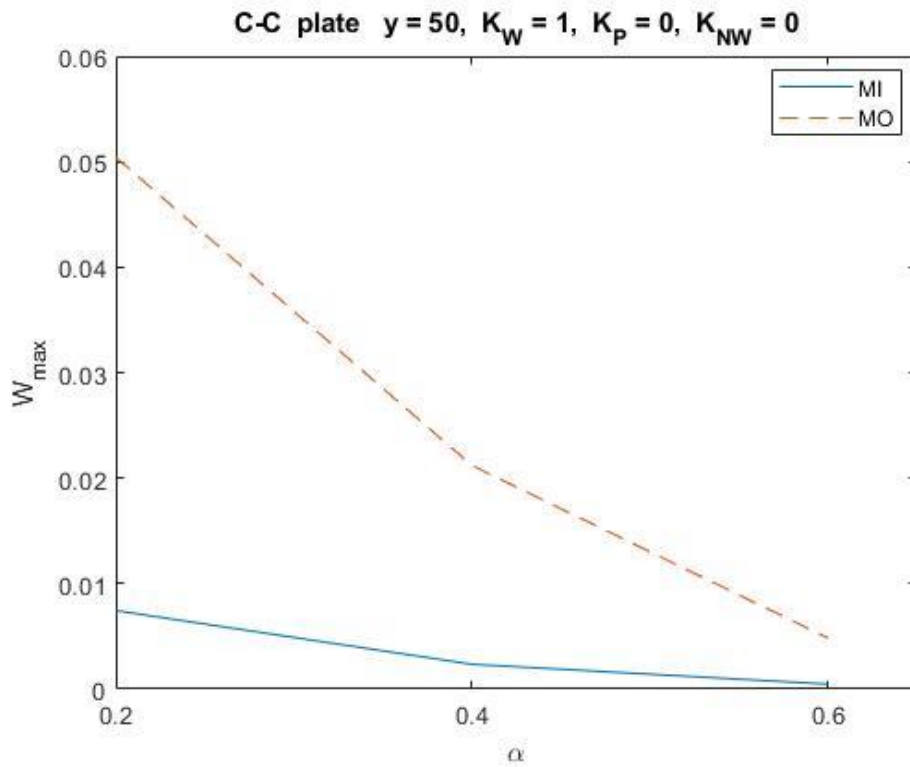


Figure A.2 Maximum deflection for different values of α

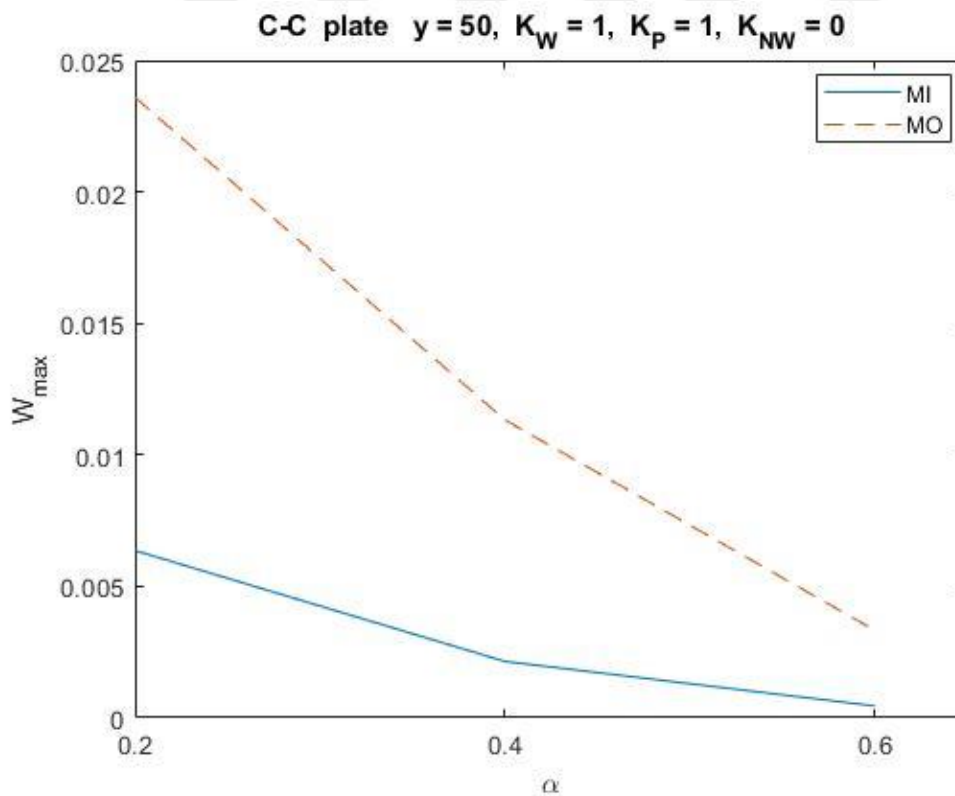


Figure A.3 Maximum deflection for different values of α

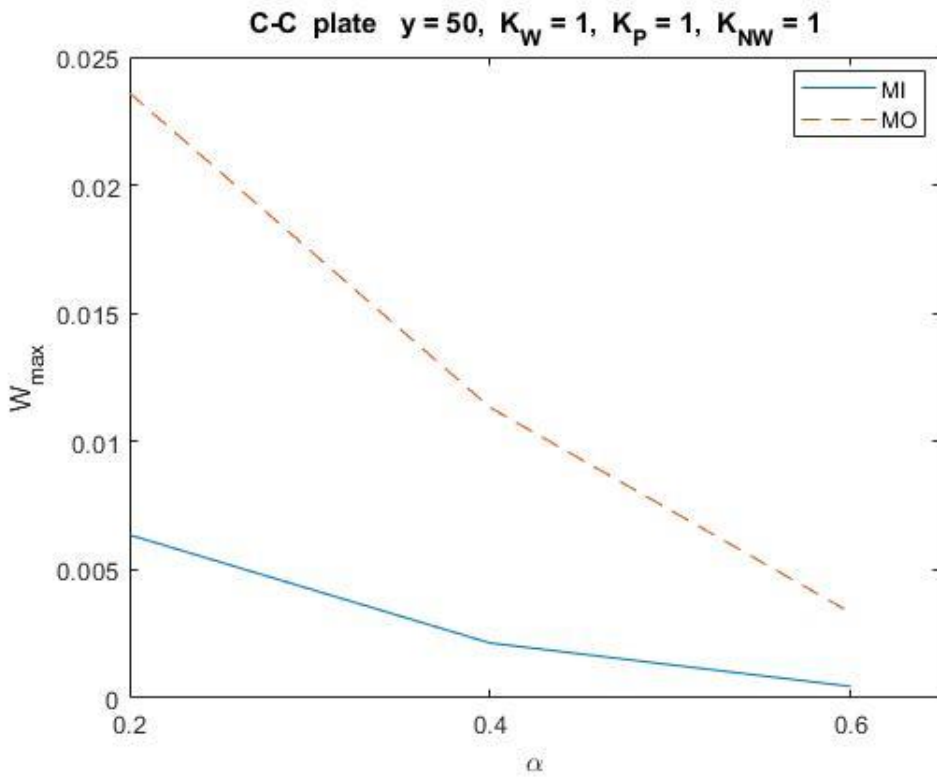


Figure A.4 Maximum deflection for different values of α

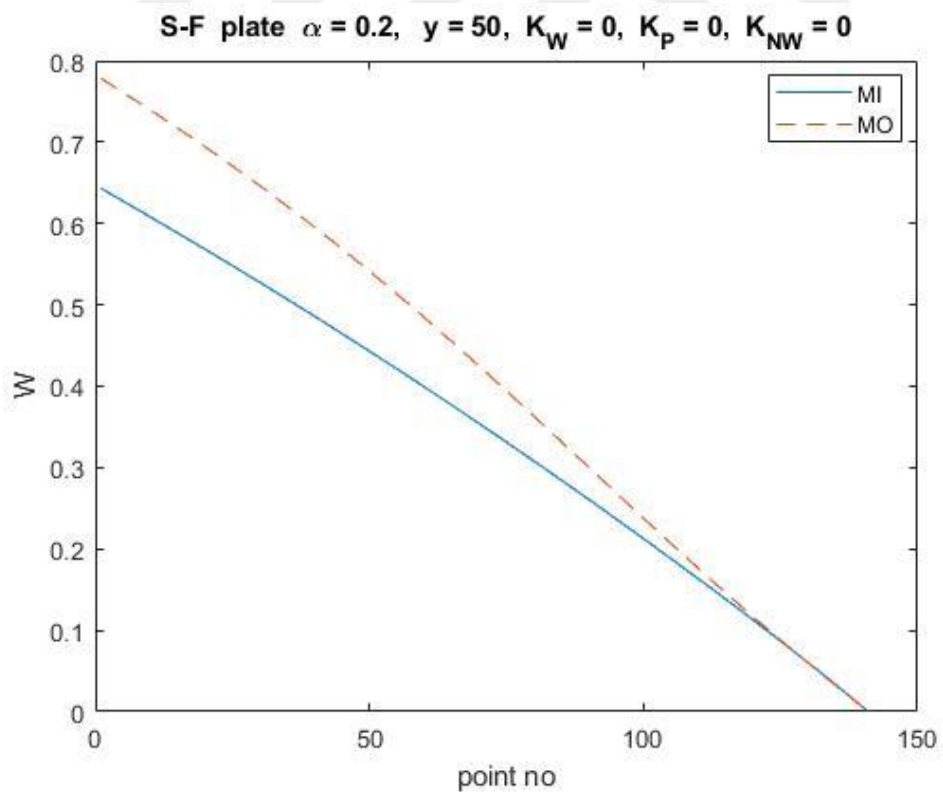


Figure A.5 Distribution of deflection along the finite difference grid

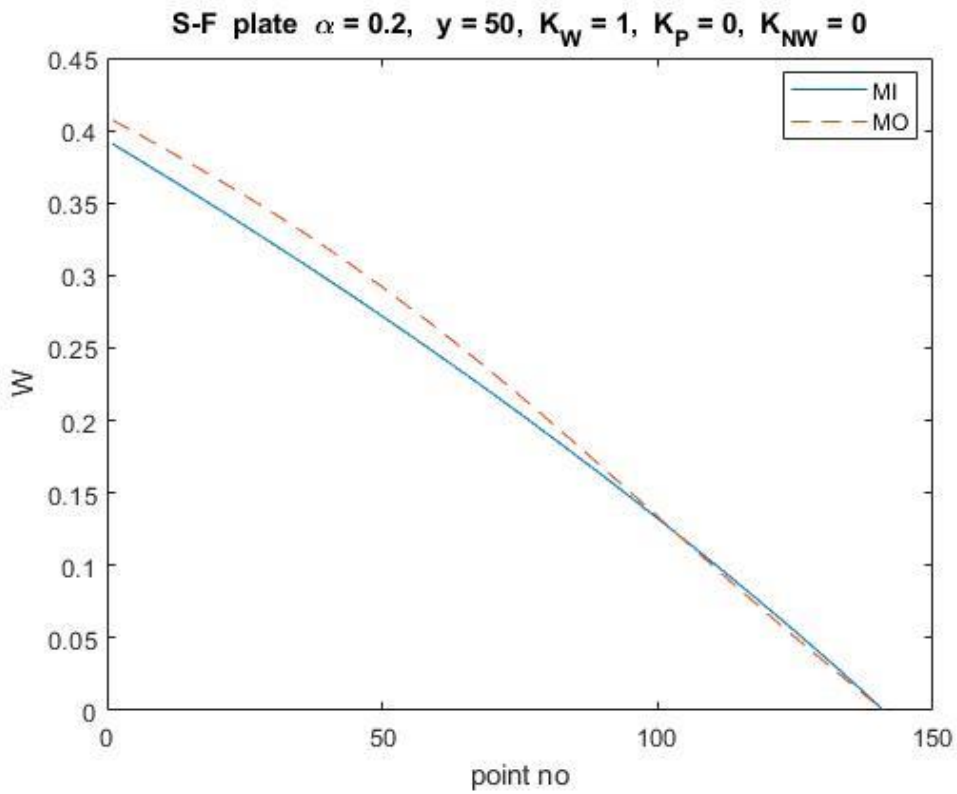


Figure A.6 Distribution of deflection along the finite difference grid

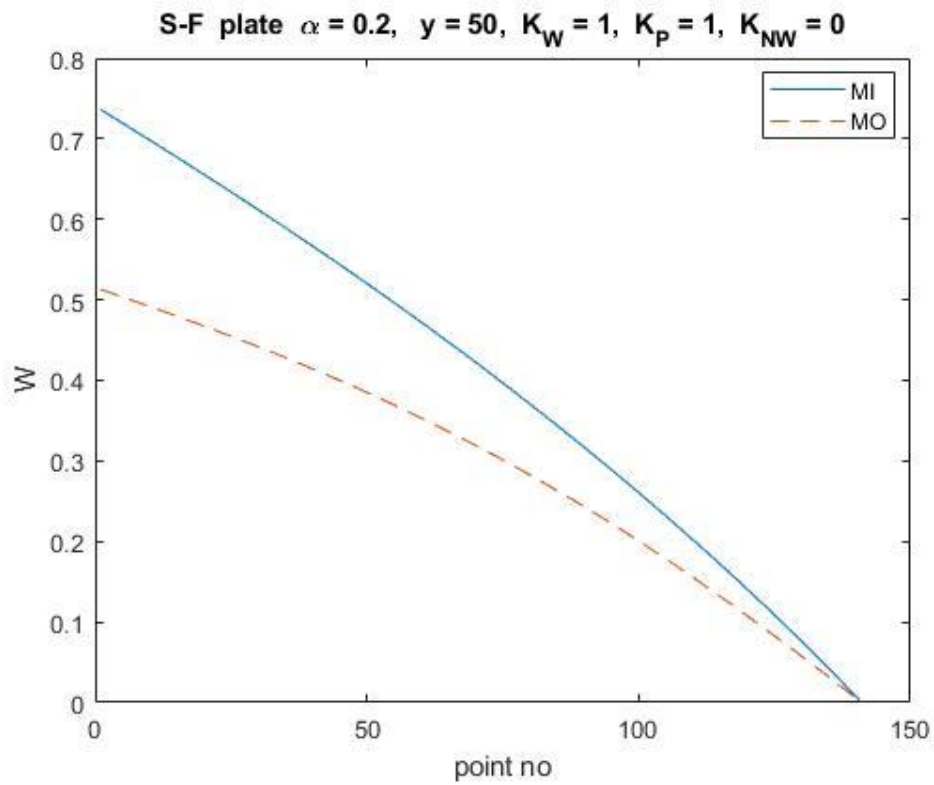


Figure A.7 Distribution of deflection along the finite difference grid

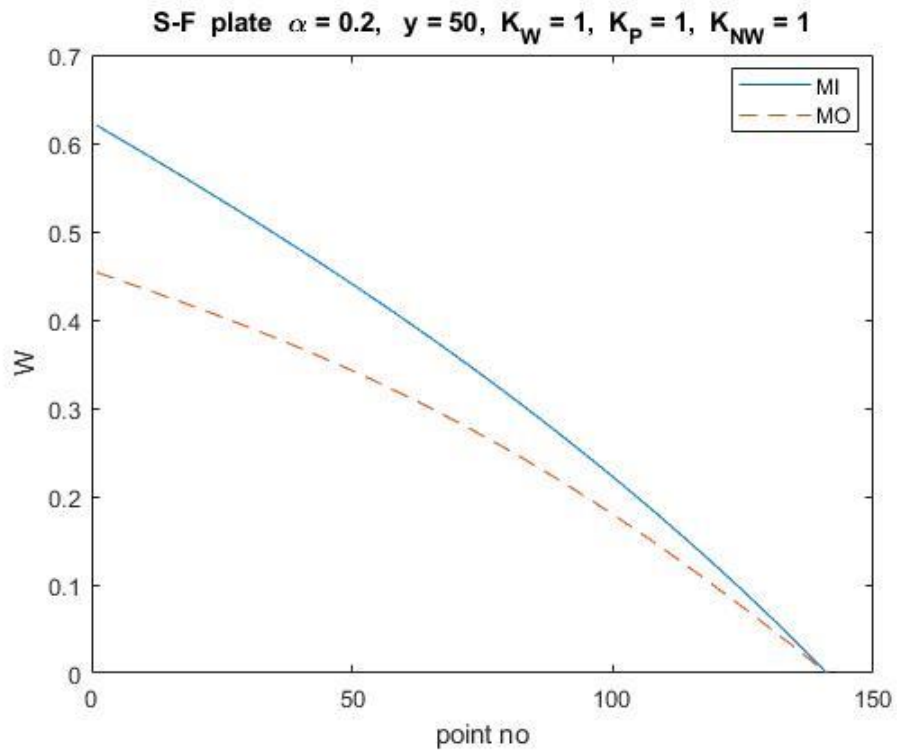


Figure A.8 Distribution of deflection along the finite difference grid

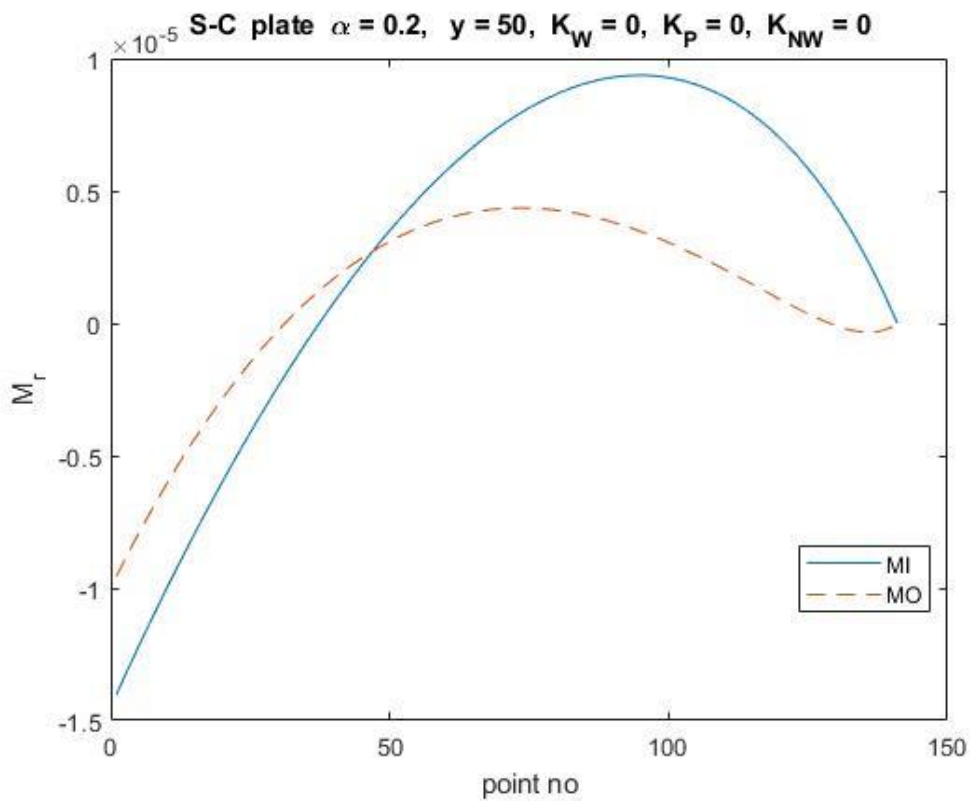


Figure A.9 Distribution of bending moment along the finite difference grid

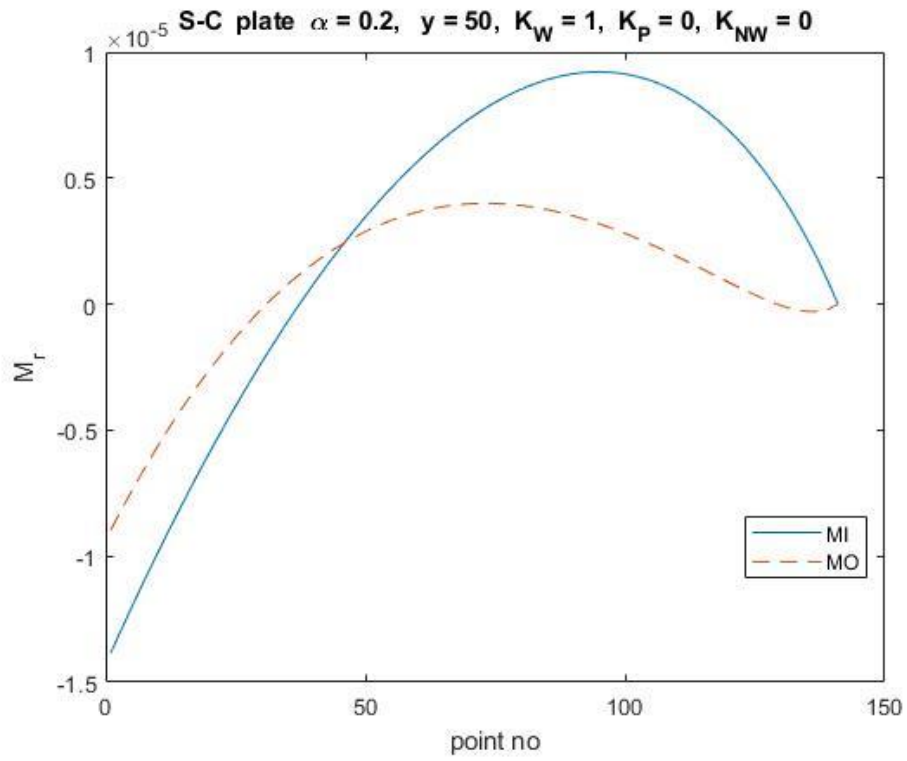


Figure A.10 Distribution of bending moment along the finite difference grid

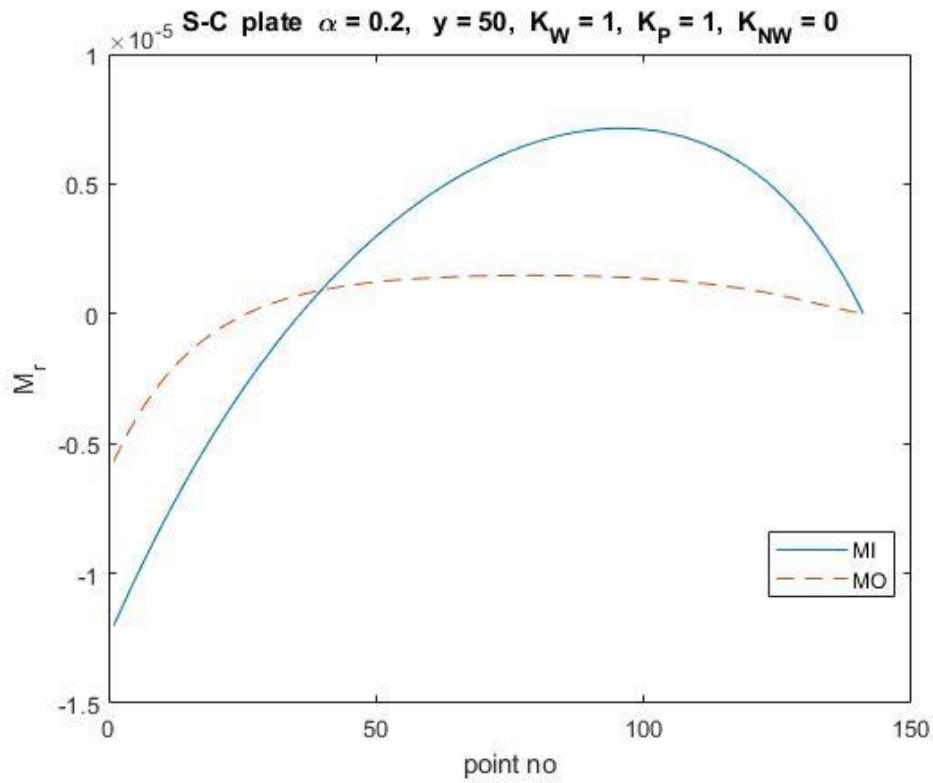


Figure A.11 Distribution of bending moment along the finite difference grid

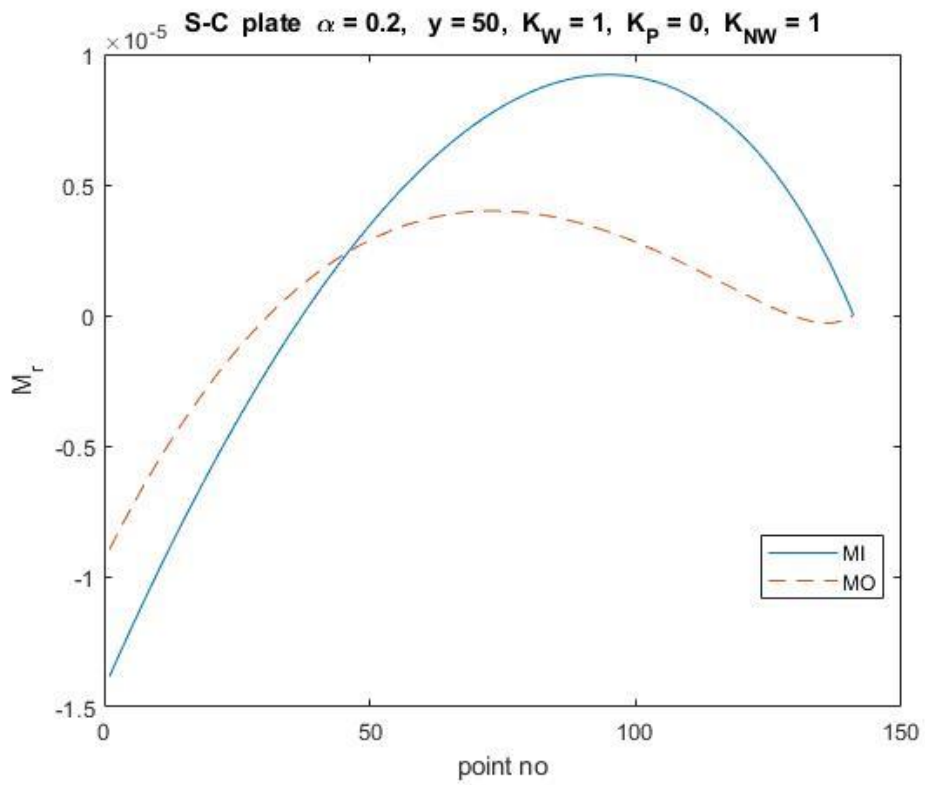


Figure A.12 Distribution of bending moment along the finite difference grid

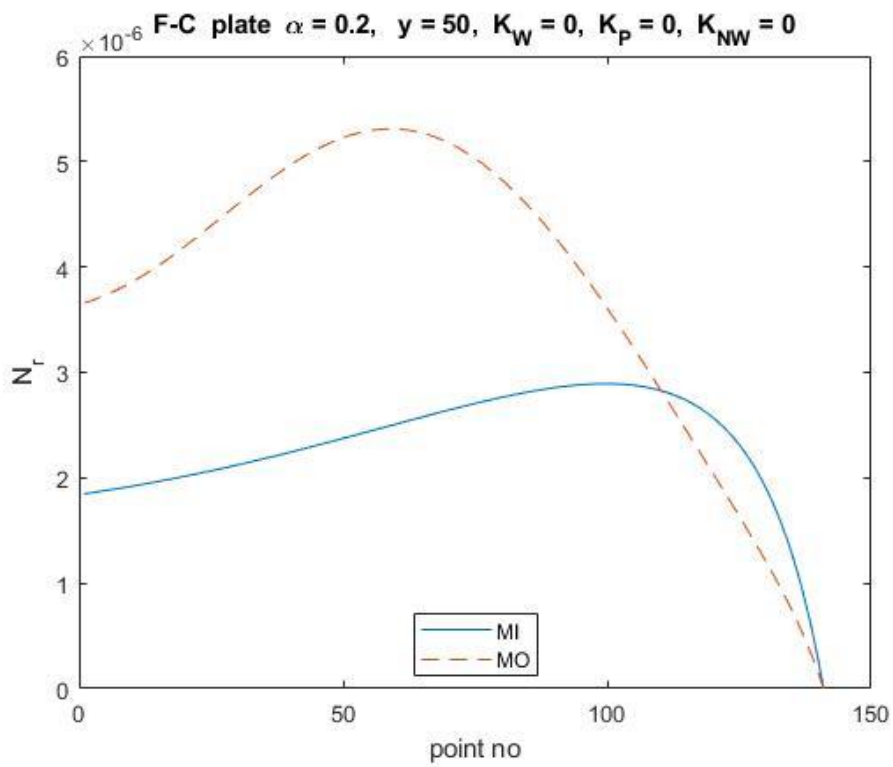


Figure A.13 Distribution of normal force along the finite difference grid

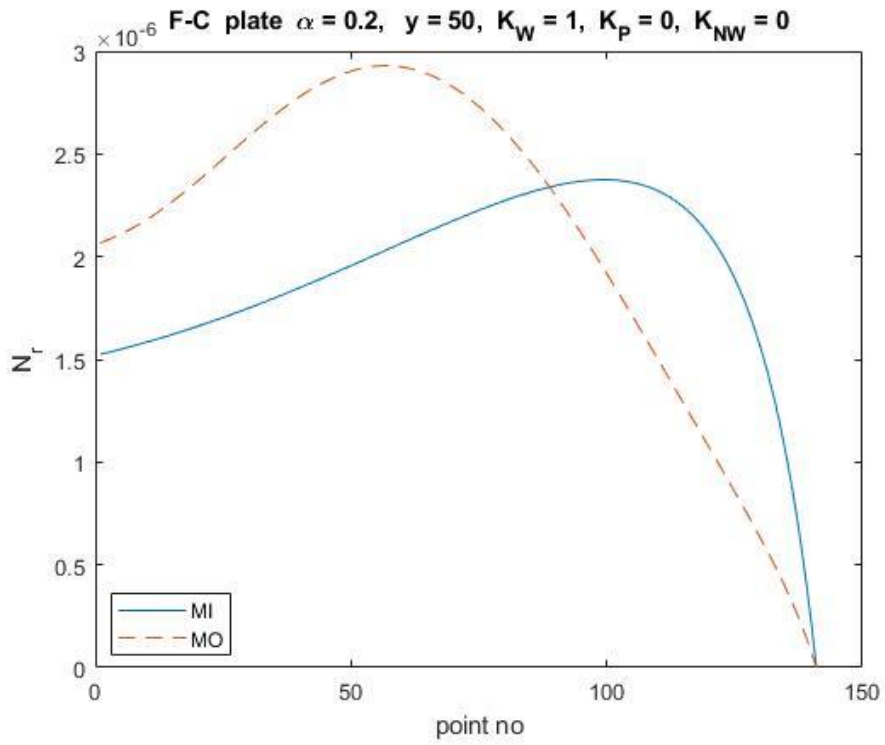


Figure A.14 Distribution of normal force along the finite difference grid

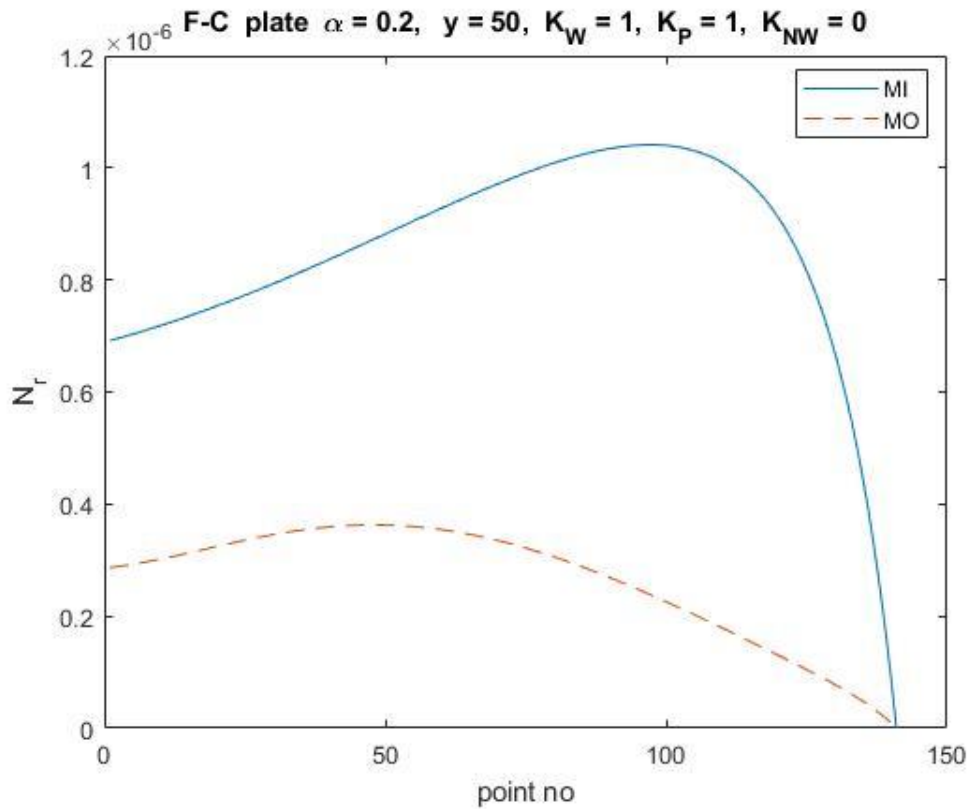


Figure A.15 Distribution of normal force along the finite difference grid

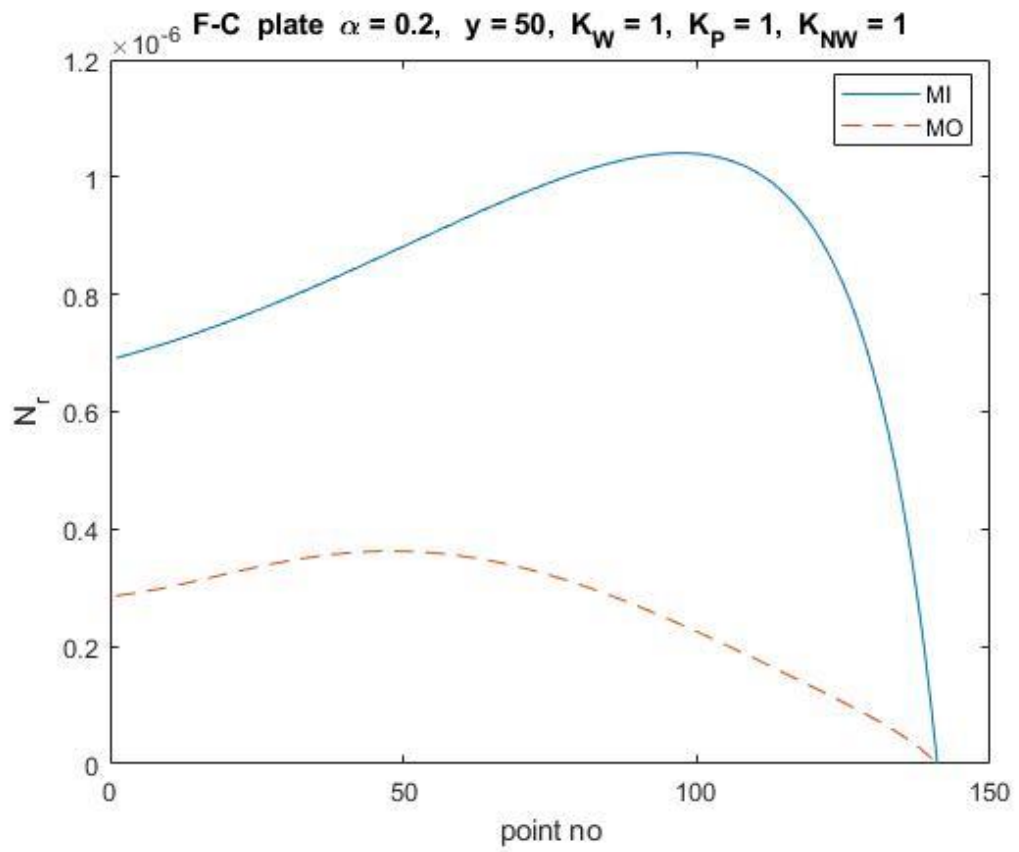


Figure A.16 Distribution of normal force along the finite difference grid

PUBLICATIONS FROM THE THESIS

Conference Presentations

1. B. Çöl and M. Altekin, “Unified Effect of the Elastic Foundation and the Material Properties on the Nonlinear Bending Response of an Annular Plate”, UBAK’23, The 16th International Scientific Research Congress - Science and Engineering, March 12, 2023, pp. 82.

